

The Feasibility of Energy Communities for Hurricane Resilience

Prateek Arora^{1,2,*} and Luis Ceferino³

¹*Civil and Urban Engineering Department, New York University*

²*Center for Urban Science and Progress, New York University*

³*Department of Civil and Environmental Engineering, University of California, Berkeley*

**Corresponding Author: pa2178@nyu.edu*

ABSTRACT

Climate extremes like hurricanes can devastate vulnerable power lines, resulting in large-scale power outages, e.g., Hurricane Beryl (2024) with 2.6 million customers in Texas, US. In response, peer-to-peer (P2P) energy sharing has emerged as a promising strategy to create energy communities (ECs) that become resilient by adopting distributed energy resources (DERs) to generate and share electricity locally, especially after disasters. We developed a validated high-fidelity model of power systems for 2,640 households, integrating geographical multi-sourced data with probabilistic risk analysis to assess the feasibility of ECs for hurricane resilience. Our study finds that ECs would have experienced shorter outages by 65.8% for Hurricane Isaias (2020) in Absecon City, New Jersey. We then utilized our power risk model to study the financial feasibility of ECs versus other measures (e.g., undergrounding lines) for resilience to future hurricanes in Absecon and compare it to Miami communities, in Florida, exposed to larger hurricanes. We show that benefits are larger in Miami, where ECs can shorten outages by 64.4%, 33%, and 50.54% than no grid upgrade, DERs without P2P sharing (non-ECs), and undergrounding. Battery backups and resilient solar panels enhanced ECs ability to operate in island mode, which would have reduced the percentage of households experiencing outages longer than a day by 74% during Hurricane Isaias (2020). Furthermore, we show that undergrounding results in a negative net present value (NPV) for communities, with households facing a 155% higher cash outflow compared to ECs, where the addition of solar panels reduces energy bills and increases savings. Our study demonstrates the importance of integrating resilience into energy policies, particularly as infrastructure evolves to meet the challenges of a changing climate.

1. INTRODUCTION

Hurricanes can destroy old and vulnerable power lines, causing large-scale cascading power failures [1, 2]. For example, (a) Hurricane Isaias (2020) caused widespread blackouts for more than 3 million customers across five states in the US [3]; (b) Hurricane Ida (2021) caused extensive damage to power infrastructure in Louisiana, leaving 1.2 million customers without power [4]; (c) Hurricane Ian (2022) left 2.7 million customers in Florida without power [5]; (d) more recently, Hurricane Beryl (2024) left more than 2.6 million customers without power in Texas [6]. These blackouts are often prolonged, threatening the health of the affected population as they endure excessive heat after a hurricane [7, 8]. Adding to the distress, the critical interdependence of transport, water pumps, medical facilities, food supplies, and emergency aids with electricity can deprive communities of critical services post-hurricane. Power outages can severely impact vulnerable community members, including households with children, the elderly, and medically

22 fragile populations [9, 10].

23 Resilient communities must have power systems capable of withstanding extreme weather events
24 and minimizing the extent of cascading power disruptions [11, 12]. In recent years, rooftop solar
25 panels have supplemented the power supply of residential, office, and industrial buildings [13].
26 The US Energy Information Administration predicts a 75% growth in solar energy production from
27 2023 to 2025 [14]. Distributed energy resources, such as rooftop solar panels, can generate electricity
28 locally and operate in island mode. Thus, DERs have great potential to enhance community
29 resilience by providing electricity access after a disaster, even when power lines fail [15].

30 Furthermore, massive governmental and industry investments are targeting integrating DERs at
31 micro-urban scales through microgrids to create energy communities (ECs), an emerging concept
32 in energy markets [16]. In ECs, prosumers - households with energy-generating sources such as
33 rooftop solar panels - sell surplus electricity under peer-to-peer (P2P) sharing to local neighborhoods
34 [17, 18]. One notable example of an energy community (EC) is the Brooklyn Microgrid, which
35 became operational in 2016 [19]. Such ECs are exhibiting resilience after large disasters. In
36 2017, Hurricane Maria battered Puerto Rico, snapping many power lines and leaving numerous
37 communities without power for several months. In response, communities have turned toward
38 building independent microgrids to solve their energy needs and resilient power infrastructure
39 [20]. To further support these initiatives, the US Department of Energy announced USD 450 million
40 in funding in July 2023 to incentivize the deployment of 30,000 to 40,000 residential solar systems
41 [20].

42 Currently, there is limited research on the benefits of resiliency with P2P sharing at the community
43 level because most studies have focused on a single or small group (2-3) of households [21–24].
44 Other studies have not considered the vulnerability of the existing grid [15]. In [25], authors showed
45 increased resilience to power outages at the household level with P2P power sharing during an
46 earthquake, but they did not consider power lines can fail during ground shaking, affecting the
47 power network connectivity of ECs. Analyzing electricity access from solar during hurricanes is
48 also more complex than for earthquakes. Unlike earthquakes, thick optical clouds during hurricanes
49 can significantly hinder the incoming solar irradiance on solar panels [26], further reducing the
50 electrical power generation during the disaster.

51 To understand the resilience of ECs, this paper develops a high-fidelity outage risk model (Hi-Fi
52 ORiM) for households with rooftop panels, behind-the-meter batteries, and P2P energy sharing
53 to predict electricity access during hurricane emergencies. The model integrates state-of-the-art
54 hurricane hazard [27], vulnerability [28], solar irradiance [29, 30], and network modeling [31] to
55 study ECs during future hurricanes with a probabilistic framework. We combine multiple data
56 streams to create a realistic synthetic network for Hi-Fi ORiM using graph theory (see Methods)
57 [31]. Thus, the Hi-Fi ORiM can assess the failure risk from each component (poles, panels) in the
58 network, as their vulnerabilities vary, and how their failures cascade through the network. We also
59 use high-performance computing to quantify uncertainties in the risk model and thoroughly study
60 the viability of adopting different resilience mitigation strategies, including ECs [32].

61 Current models that evaluate the viability of DERs in high hurricane hazard areas do not account
62 for solar panel failures, solar irradiance reductions, or the long duration of power recovery during
63 large hurricanes. These factors are crucial for evaluating the ability of DERs to sustain electricity
64 supply during disasters. Existing tools, such as renewable energy integration and optimization
65 tools (REopt) and solar power calculators (PVwatts), do not consider solar panel failure risks,
66 neglecting their repair and replacement costs when optimizing panel and battery size for savings
67 and resilience [33]. Other important studies for hurricane resilience have also neglected such failure
68 risks, in addition to significant solar irradiance decays during hurricanes [34]. Rooftop solar panels
69 can have a 75% failure probability for hurricanes with wind speeds over 90m/s [35]. An example

70 of a failed solar panel in the aftermath of Hurricane Ian (2022) is shown in Supplementary Figure
71 S5. Additionally, in [26], the authors found that solar generation could decrease by more than 70%
72 in Miami-Dade, US, during category-4 hurricanes. Moreover, scholars have mostly considered a
73 particular outage scenario with quick recoveries of 8h to 24h [23, 36]. However, hurricanes can
74 leave populations without power for days to months [10].

75 Other grid-hardening measures can also increase the resilience of power systems. For example,
76 the resilience of the power grid to hurricanes can be enhanced by undergrounding overhead power
77 lines [37–39]. However, the cost of undergrounding can be high and result in increased consumer
78 electricity tariffs [38]. On the contrary, there is growing literature on the economic and financial
79 benefits, in addition to the environmental ones, that renewables can bring to reduce the billions of
80 dollars in losses caused by power blackouts [21, 36, 40, 41]. Thus, evaluating and comparing the
81 cost of adopting such mitigation strategies to enhance resilience becomes essential.

82 This paper presents and develops a high-fidelity risk outage model (Hi-Fi ORiM) of a distribution
83 grid serving 2,640 households. We calibrate the model with power outage and recovery data from
84 Hurricane Isaias (2020) to serve as a validated test bed for assessing the resilience of power
85 communities prone to hurricane risks. To evaluate the finances of resilient electricity, we determine
86 the net present value (NPV) of solar panel adoption by considering installation costs, cash flows
87 (amount of electricity sold and bought), and the value of resilience [42]. Traditionally, value of
88 resilience is considered by multiplying the avoided outage duration with the value of lost load
89 (VoLL), expressed in dollars per kWh of unserved load [42, 43]. However, traditional VoLL is limited
90 to qualitative analysis as it is determined through surveys based on the responses to hypothetical
91 conditions provided to the responder. This paper presents a new method to quantify the value
92 of resilience by arranging alternative energy resources during emergencies. Our study compares
93 multiple strategies for resilient electricity: (a) ECs, which involves the adoption of solar panels with
94 P2P sharing; (b) non-ECs, which involves the adoption of solar panels without P2P sharing; and
95 (c) undergrounding of power lines. Additionally, we integrate 5,018 synthetic hurricanes from a
96 state-of-the-art hurricane hazard model to study the resilience benefits against future hurricanes
97 [44]. Our combined approach of state-of-the-art Digital Twin, probabilistic risk modeling, and
98 financial analysis would allow stakeholders such as homeowners, utilities, and local governments
99 to make informed decisions and invest in building a resilient power grid for the future.

100 2. RESULTS

101 A. Validated High-Fidelity Outage Risk Model of Power Network

102 The high-fidelity outage risk model (Hi-Fi ORiM) represents the physical systems of the power grid,
103 enabling simulations of their interactions with natural hazards [31, 45]. This approach assesses the
104 vulnerability of entire power networks by integrating risk modeling for individual components
105 with their interconnections rather than focusing on single components. This method is particularly
106 valuable in scenarios where network dynamics are crucial, such as in power networks. We lever-
107 aged high-performance computing (HPC) resources to overcome the computational challenges of
108 running multiple power systems and hurricane scenarios.

109 We developed Hi-Fi ORiM of the power distribution network serving 2,640 residential consumers
110 in Absecon City in Atlantic County, New Jersey, who could benefit as ECs. We integrated informa-
111 tion from publicly available multi-sourced datasets in the model (Figure 1), including limited pole
112 locations from OpenStreetMaps [46], roads and building parcels from New Jersey Open Geographic
113 Information Systems [47, 48], and building footprints from Microsoft [49].

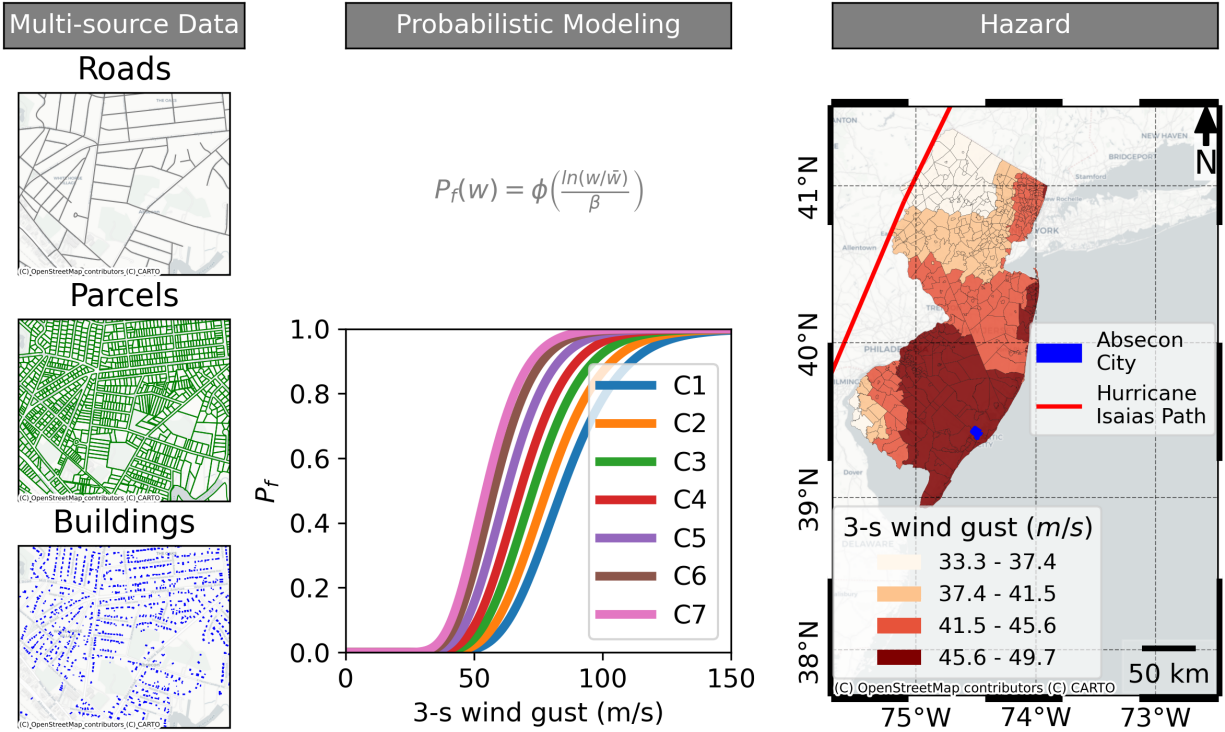


Fig. 1. Hi-Fi ORiM developed using open-source datasets of roads, parcels, and buildings from the New Jersey Geographic Information Network [50]; fragility curves for pole failure probabilities across classes C1-C7, modeled with a log-normal distribution for a median 3-second wind gust (\bar{w}) and dispersion (β) [28] (see Methods); and hazard information from 3-second wind gusts during Hurricane Isaias (2020).

114 Most distribution networks in the US have a radial structure, where the failure of a single over-
 115 head pole can cause cascading power failures for all downstream consumers [51]. We developed the
 116 Hi-Fi ORiM by reproducing such a radial topology and coupling it with hazard and vulnerability
 117 models of the power system's components [31]. The resulting probabilistic risk-network model
 118 predicts the damage to the overhead poles from wind hazards, disconnections in the power network
 119 due to damages, and the recovery of damaged components back to a fully connected network (see
 120 Methods). We only consider wind-driven failures of distribution poles [31] and do not model the
 121 compound failures from falling trees on distribution poles due to lack of data [52]. Fragility curves
 122 define the wind-dependent failure probabilities for different classes of poles (Figure 1). We used a
 123 full circulating [27] and background [53] wind model to capture the complete structure of tropical
 124 cyclones to assess realistic hurricane winds. Figure 1 presents all the components to build a Hi-Fi
 125 ORiM, including datasets, risk modeling, and hazard information.

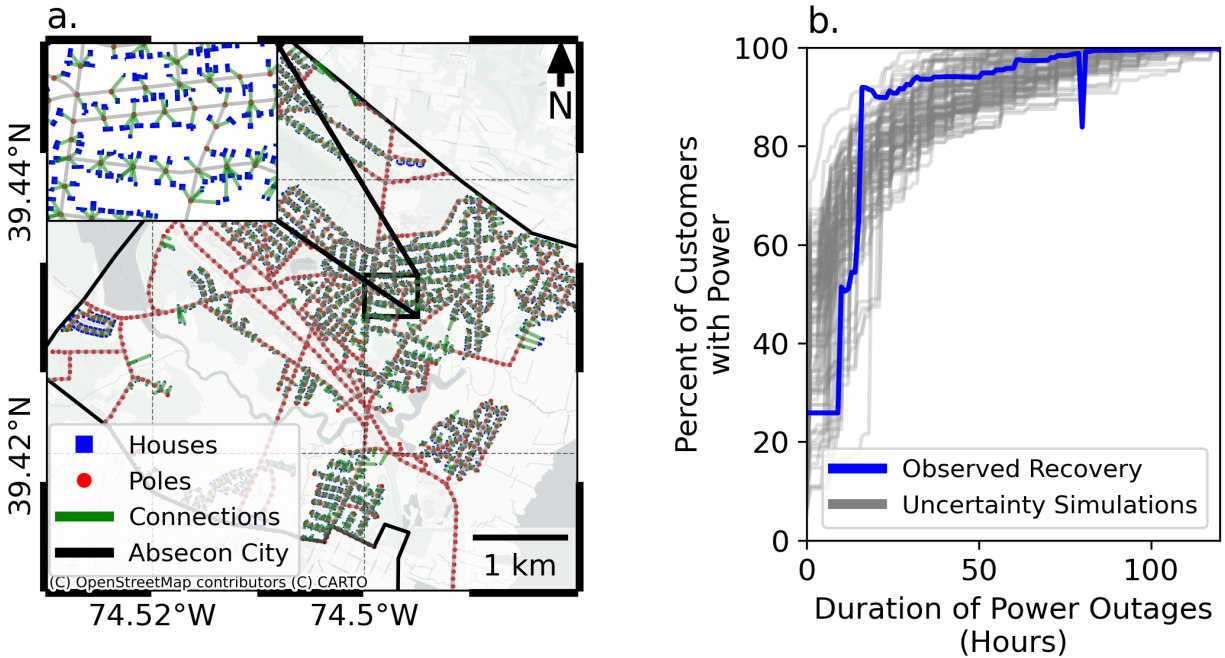


Fig. 2. a. Representation of constructed synthetic grid for Absecon City, New Jersey. **b.** Recovery simulations of Hi-Fi ORiM calibrated for the observed recovery during Hurricane Isaias (2020).

126 Our Hi-Fi ORiM was calibrated using outage and recovery data from Hurricane Isaias (2020)
 127 (see Methods) [54]. Isaias carried winds close to 100-year return period events for New Jersey [55].
 128 Even though Isaias transitioned to a tropical storm before hitting New Jersey, it still snapped power
 129 lines and destroyed many power poles [56]. Isaias caused economic losses of 4.2 billion and 15
 130 deaths and was responsible for major blackouts across five states in the Northeast United States.
 131 One million customers were without power alone in New Jersey, with many suffering power loss
 132 for over four days [57, 58].

133 Our developed Hi-Fi ORiM model, as shown in Figure 2a, can simulate hurricane-induced
 134 outages and the post-disaster recovery of the power network with high precision, as demonstrated
 135 in Figure 2b. Our model predicts maximum percent outages of 77.42% close to the observed percent
 136 outages for 74.15% of consumers. In our synthetic grid, 95% of the customers recover in 61 hours
 137 close to 55 hours for the observed recovery of the power grid in Absecon City. Our developed Hi-Fi
 138 ORiM model represents a typical suburban power network, making our framework adaptable for
 139 assessing the risk of power outages across varying levels of hurricane wind intensity, from low to
 140 high.

141 **B. Could we have enhanced electricity resilience during Hurricane Isaias?**

142 We found that communities would have benefited significantly from resilience measures during
 143 Hurricane Isaias (Figure 4). To compare the effectiveness of resilience measures, we considered
 144 four different cases: (a) No Upgrade, (b) ECs, (c) Non-ECs, and (d) Underground power lines. We
 145 ran 400 random simulations of our probabilistic risk model during Hurricane Isaias.

146 The US is projected to have 55% of its electricity generation through solar energy [59]. In line with
 147 this projection, we assumed that 50% of houses in a cluster would adopt solar panels and battery
 148 storage of 10 kWh. We grouped the houses into clusters based on Euclidean distance to study
 149 the effectiveness of energy sharing (see Methods). The solar panels are sized for net-zero energy

150 consumption, *i.e.*, energy generated by panels equals energy consumed by households. Figure
 151 3a. depicts a network of houses in a power grid without solar panels, where all the houses lose
 152 power during hurricane emergencies. In contrast, another network in Figure 3b. has prosumers
 153 installing rooftop solar panels. These prosumers can generate electricity or use backup power from
 154 a battery during a hurricane emergency. The prosumers gain resilience through solar panels and
 155 can enhance the community's resilience by sharing excess electricity in a solar EC.

156 To model ECs, we extended our Hi-Fi ORiM model (Figure 8). First, we integrated solar panel
 157 vulnerability functions into our risk model [35] to predict damage from the hurricane winds [27, 53]
 158 We integrated a stochastic model to predict reduced solar irradiance into the Hi-Fi ORiM model,
 159 using historical solar data to capture the effect of thick hurricane clouds on solar generation, as
 160 shown in Supplementary Figure S4 (see Methods) [26]. Finally, we modeled each household's
 161 recovery based on the available solar irradiance and undamaged network components.

162 To study the effectiveness of undergrounding measures, we assumed that 50% of the most
 163 vulnerable power poles are buried. For example, class 7 poles, which have the lowest median wind
 164 threshold on the fragility curve (Figure 1), are undergrounded first, followed by the second most
 165 vulnerable poles.

166 Supplementary Figure S7 shows the adoption of solar panels among prosumers across Absecon
 167 City for ECs and non-ECs grid hardening configurations, as well as the undergrounding of power
 168 poles (lines) to increase resilience against strong winds (see Methods).

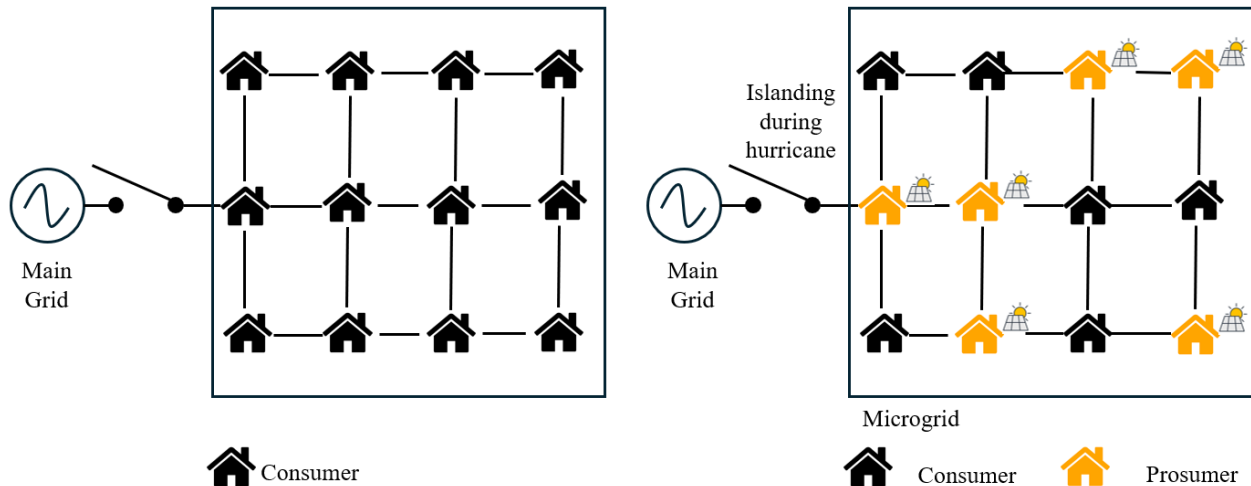


Fig. 3. Schematic Diagram of the P2P energy sharing. The left figure shows the traditional grids where consumers suffer outages during hurricanes due to extensive damage to the power grid, and the right figure shows the adoption of solar panels so that the prosumers can generate electricity in island mode after the hurricane and share excessive energy with consumers (without solar panels) to increase the resilience against power outages.

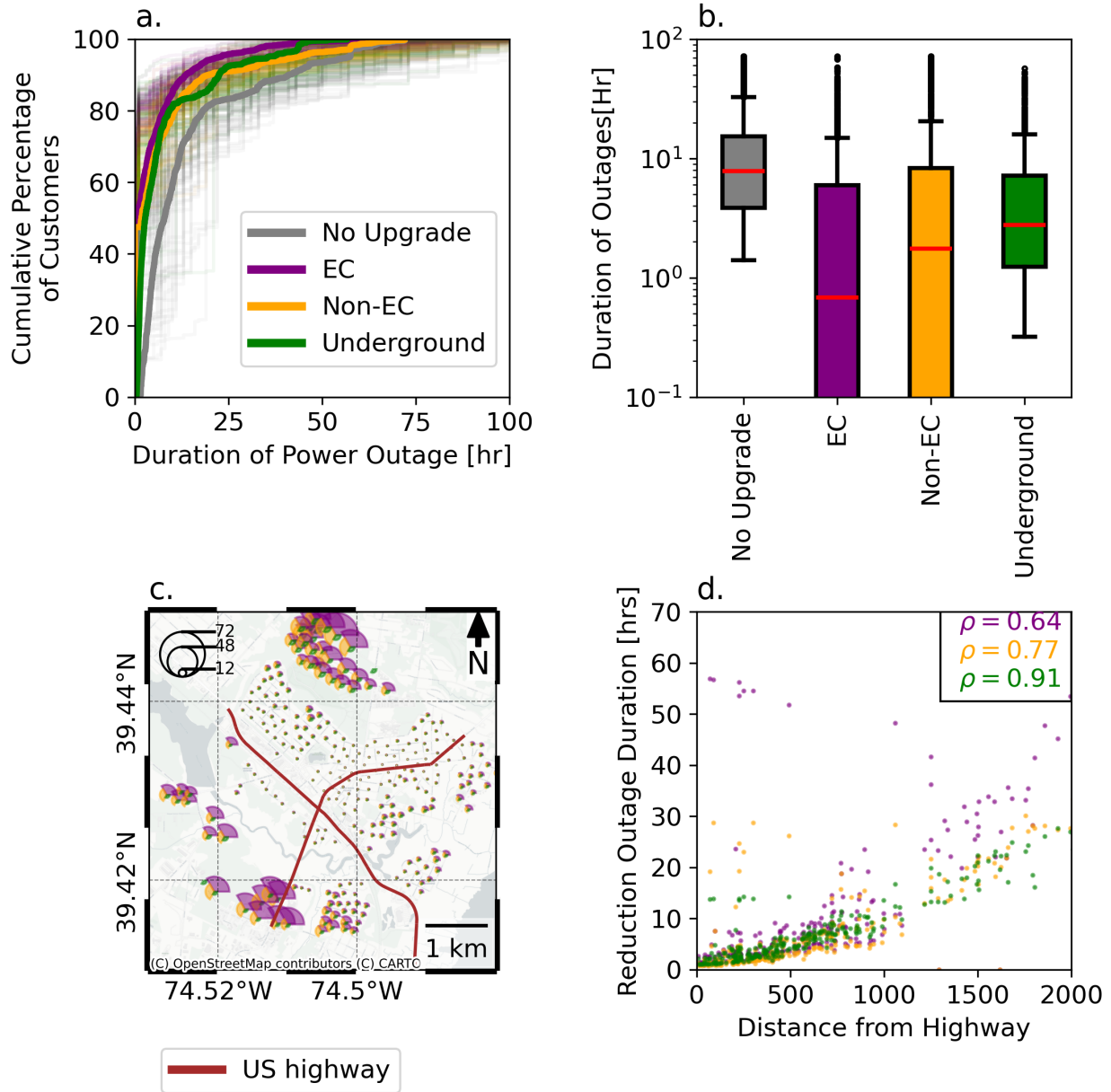


Fig. 4. Simulations for resilient strategies scenarios for the developed Hi-Fi ORiM in Absecon City, New Jersey, during hurricane Isaias (2020). **a.** Cumulative percentage of customers experiencing power outages. **b.** Duration of mean power outages observed for each household under different configurations of Hi-Fi ORiM **c.** Representation of mean reduction in the duration of power outages for a cluster for different resilience strategies compared to the base case of no upgrades. **d.** Scatter plot between the reduced number of outages for a cluster and distance from the US highway.

169 IEEE Standard 1366-2022 defines reliability indices, such as the System Average Interruption
 170 Frequency Index (SAIFI). As reliability only focuses on daily interruptions, utility performance
 171 ratings exclude catastrophic events, defined as 'Major Day Events,' such as hurricanes, from SAIFI
 172 calculations [60]. Thus, no standard index is defined for measuring the resilience of power systems.

173 However, any interruption to the consumers is a disturbance, whether caused by a daily outage or a
 174 hurricane. The IEEE Power and Energy Sector (PES) Task Force emphasizes the resilience of power
 175 systems as the ability to limit the extent, system impact, and duration of degradation following
 176 an extraordinary event such as natural hazards [12]. Thus, we identify the resilience gained from
 177 resilience strategies as the reduction in outage durations. Our proposed resilient strategies focus
 178 on reducing outage durations by increasing the robustness of power systems through integrating
 179 DERs and undergrounding power lines.

Configuration	Outages duration (hours)	Households (%) with long outages [≥ 24 hours]
No Upgrade	13.92 [1.61-59.86]	16.86% [8.41%-31.45%]
ECs	4.76 [0.00-33.11]	4.43% [2.50%-11.33%]
Non-ECs	7.41 [0.00-57.56]	9.05% [4.61%-16.45%]
Underground	7.46 [0.53-43.59]	8.41% [4.50%-20.76%]

Table 1. Mean outage duration of households and households with longer outages for the scenario of Hurricane Isaias (2020)
 *95% C.I. in bracket

180 Our results (Figure 4a-b and Table 1) show that ECs would achieve the highest resilience against
 181 hurricanes compared to non-ECs and undergrounding configurations in the scenario of Hurricane
 182 Isaias (2020). We found that households in ECs would experience a mean outage duration of
 183 4.76 hours per household, which is 65.80%, 35.76%, and 36.19% shorter than in the no upgrade,
 184 non-ECs, and undergrounding cases, respectively. Moreover, 97.5% of households in ECs would
 185 have an outage duration of less than 33.11 hours, whereas no-upgrade scenario would be 80.80%
 186 longer. Additionally, ECs would have a mean of 4.43% of households experiencing long outages
 187 (> 24 hours), which is 73.47%, 51.04%, and 47.32% less than in the no-upgrade, non-ECs, and
 188 undergrounding cases, respectively. At the 97.5th percentile, ECs would have 11.33% of households
 189 experiencing long outages, which is 177.58% higher in the no upgrade case.

190 We show the spatial distribution of mean reductions in power outage duration for different
 191 resilience strategies across 264 clusters, comprising 2,640 households, in Figure 4c. We observe more
 192 significant reductions in outage durations farther from the main highway across all mitigation cases
 193 (Figure 4d). For instance, clusters in ECs between 1000 and 1500 meters would observe an average
 194 reduction in outage duration of 24.53 hours, three times higher than the reduction for clusters
 195 between 500 and 1000 meters. Typically, power grids are restored using a top-down strategy where
 196 repair teams reach the poles closer to the main highway first [61, 62]. Thus, households with more
 197 remote access through local roads often recover electricity last, especially in radial distribution
 198 networks. Our results show that these resilience measures, and especially ECs, can significantly
 199 enhance electricity access for such households (Figure 4d).

200 C. Assessing the effectiveness of resilience measure to future hurricanes

201 Hurricane Isaias reached a maximum category of 1, but the US is exposed to more significant
 202 events, e.g., the recent 2024 category 5 Hurricane Beryl with 165 mph winds [63]. To analyze the
 203 benefits of resilience measures comprehensively, we studied multiple realistic hurricane scenarios
 204 using state-of-art hurricane hazard models [27]. We analyzed 5,018 landfalling hurricanes that

205 originate in the North Atlantic Basin [64] representing the hurricane hazard under the current
206 climate scenario (Figure 5a). These hurricanes cover approximately 1,485 years, as about 3.38
207 hurricanes from the Atlantic Basin make landfall each year [35]. We sampled the hurricanes yearly
208 as a random Poisson process (see Methods). We represent a typical year as the mean of 1,485 years
209 of simulations. We ran a total of $\sim 4 \times 10^5$ simulations to model outages and recovery in Absecon
210 and Miami.

211 We also considered a different region from Absecon City to evaluate how resilience measures
212 apply to other US communities exposed to the largest hurricane hazards. To do so, we leveraged our
213 Hi-Fi ORiM model, which represents typical communities with radial distribution lines in the US,
214 to also analyze communities in Miami, Florida (Figure 5a). Miami has recently experienced strong
215 hurricanes *e.g.*, Matthew (2016), Irma (2017), Dorian (2019), Ian (2022) and can experience winds
216 of 62 *m/s* for a 100-year return period, which is 38% higher than 45 *m/s* winds for Absecon City.
217 Notice that wooden power poles can sustain winds up to 20 *m/s* [65]. Thus, wind speeds beyond
218 20 *m/s* can make them fail. In Absecon City, only 5.14% simulations exceeded 20 *m/s* (Figure
219 5b). In contrast, Miami has 20.18% simulations that exceeded 20 *m/s* (Figure 5c), highlighting
220 significantly higher hazards due to its different location (Figure 5a).

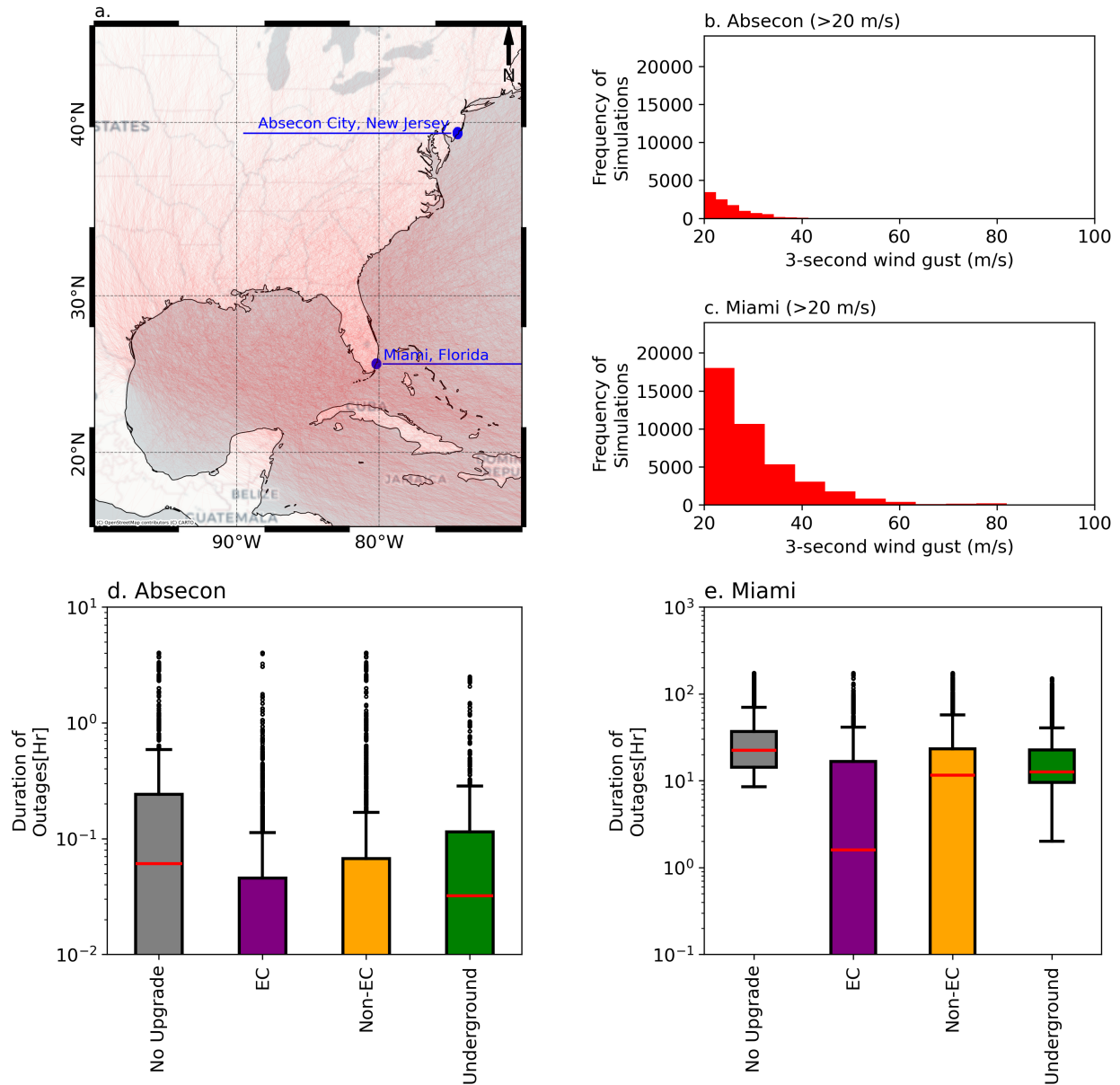


Fig. 5. Simulations for the future (synthetic) hurricanes. **a.** Tracks of synthetic hurricanes in the North Atlantic basin based on the historical climate [44]. **b.** Distribution of wind speeds (>20 m/s) in Absecon City, New Jersey. **c.** Distribution of wind speeds (>20 m/s) in Miami, Florida. **d.** Average duration of power outages observed for each household under different configurations of Hi-Fi ORiM in Absecon City, New Jersey, for 25 years. **e.** Average duration of power outages observed for each household under different configurations of Hi-Fi ORiM in Miami, Florida, for 25 years.

221 We investigated the same four cases, including a baseline and three resilience measures, under
 222 future hurricanes. The average lifetime of a solar project is 25 years. We also assumed that utilities
 223 would recover undergrounding costs over 25 years. Thus, we present the average duration of
 224 power outages for each house across 25 years with different power grid configurations in Figures
 225 5d-e and Table 2.

226 Similar to the results for Hurricane Isaias (2020), we found that households will gain more
 227 resilience in ECs. From Figure 5d, we observe that the low-wind region of Absecon City would
 228 have minimal outages across all the configurations. The observed outages for the high winds region
 229 of Miami are ~ 100 times more than the low wind region of Absecon City. In an extreme case, a
 230 household can observe an outage of 206 hours (8 days) in Florida. In the aftermath of Hurricane
 231 Ian (2022), a category 4 hurricane, nearly 30% of Lee County in Florida consumers were without
 232 power after 8 days.

233 We observe more significant resilience gains for Miami than for Absecon City. For instance,
 234 the mean outage durations in Miami decreased from 35.64 hours in the no upgrade scenario
 235 to 12.69 hours with ECs, compared to a smaller reduction in Absecon, where the mean outage
 236 durations dropped from 0.31 hours to 0.08 hours. The biggest improvement in resilience for
 237 Miami is observed with ECs, where we observe a 64.4%, 33.0%, and 50.5% average reduction in
 238 outage duration compared to the no-upgrade, non-ECs, and undergrounding cases, respectively.
 239 Additionally, 97.5% of households in Miami will observe an average outage duration of less than
 240 80.17 hours, which is 126.32% higher than the outage duration of 130.66 hours for the no upgrade
 241 case. Finally, we also observe an increasing reduction in duration with the distance from the
 242 highway (Supplementary Figure S9). Like the scenario analysis for Hurricane Isaias, resilience
 243 gains are maximized for the population at greater risk of prolonged power outages.

Location	Configuration	Outages duration (hours)
Absecon	No Upgrade	0.31 [0.00-2.90]
Absecon	ECs	0.08 [0.00-0.69]
Absecon	Non-ECs	0.17 [0.00-2.34]
Absecon	Underground	0.08 [0.00-1.45]
Miami	No Upgrade	35.64 [11.42-147.09]
Miami	ECs	12.69 [0.00-80.17]
Miami	Non-ECs	18.95 [0.00-139.43]
Miami	Underground	25.63 [7.40-128.24]

Table 2. Mean outage duration of households (95% C.I. in bracket)

244 **D. Household-scale resilience financing**

245 Here, we quantify the finances for the resilience measure to weigh the cost of investments against
 246 the benefits [66]. We evaluate the profitability of prosumers by determining their net present value
 247 (NPV) for 25 years, i.e., the solar panel’s lifespan (see Methods). We studied the contributions of
 248 different components towards NPV: (a) investments and operation costs for panels and batteries
 249 (I&O), (b) savings from not purchasing grid electricity, (c) additional state incentives, (d) panel
 250 damage from winds, and (e) the avoided costs from shorter/no outages.

251 Previous research [42] has considered the financial value of resilience measures as the savings
 252 from avoided outages based on the value of lost load (VoLL). Historically, the VoLL for residential
 253 customers has been estimated using questionnaires based on hypothetical outage scenarios [43].

254 These questionnaires ask about customers' willingness to pay to avoid outages, but the wide range
255 of options, such as 0 to 50 USD, can lead to underestimations of VoLL as customers tend to choose
256 a lower value. Additionally, these surveys consider outages of up to 16 hours, whereas hurricane-
257 related outages can last up to a week. In contrast, we quantified the value of avoided outages as the
258 savings from not needing alternate energy sources, such as emergency diesel generators, to supply
259 electricity when the grid is down (see Supplementary Text S3). Many communities use generators
260 for days or even weeks as a backup during significant power outages, for example, in Florida after
261 Hurricane Irma (2017) [7]. Thus, we use this avoided cost as a more realistic way to quantify the
262 value of shorter outages during disasters.

263 We define profitable prosumers as those with a positive NPV and study the effects of state
264 incentives. For brevity, we show results for NPV with state incentives here (Figure 6a) and without
265 them in the Supplementary Information (Figure S11 and S12). Prosumers are more profitable
266 in Miami as Florida receives nearly 25% more solar irradiance than New Jersey (Supplementary
267 Figure S3) [29]. Smaller-sized rooftop solar systems can generate the same amount of solar energy
268 in Florida as larger-sized solar panel systems in New Jersey. Figures 6b-c represent the breakdown
269 of profitable and unprofitable prosumers in Absecon City and Miami. While profitable prosumers
270 have similar I&O costs in Miami and Absecon City, prosumers in Miami have higher savings than
271 those in Absecon City. For example, profitable prosumers in ECs have 29% higher savings in Miami
272 than in Absecon City. We found that 99% of the prosumers are profitable in Miami compared to
273 92% in Absecon for both ECs and non-ECs.

274 Our findings show that, on average, the value of resilience, measured as the avoided cost from
275 outages, is about 16% and 23% of I&O costs for profitable and unprofitable prosumers, respectively
276 (Figure 6b-c). These avoided costs are important and can supplement other savings from reduced
277 grid electricity purchases and energy sharing. On average, prosumers have higher profits and
278 savings with ECs configuration than non-ECs. This can be attributed to higher selling electricity
279 costs in local energy markets than net-metering rates. The median NPV with state incentives in
280 Absecon and Miami for ECs is 16% and 7% higher than for non-ECs.

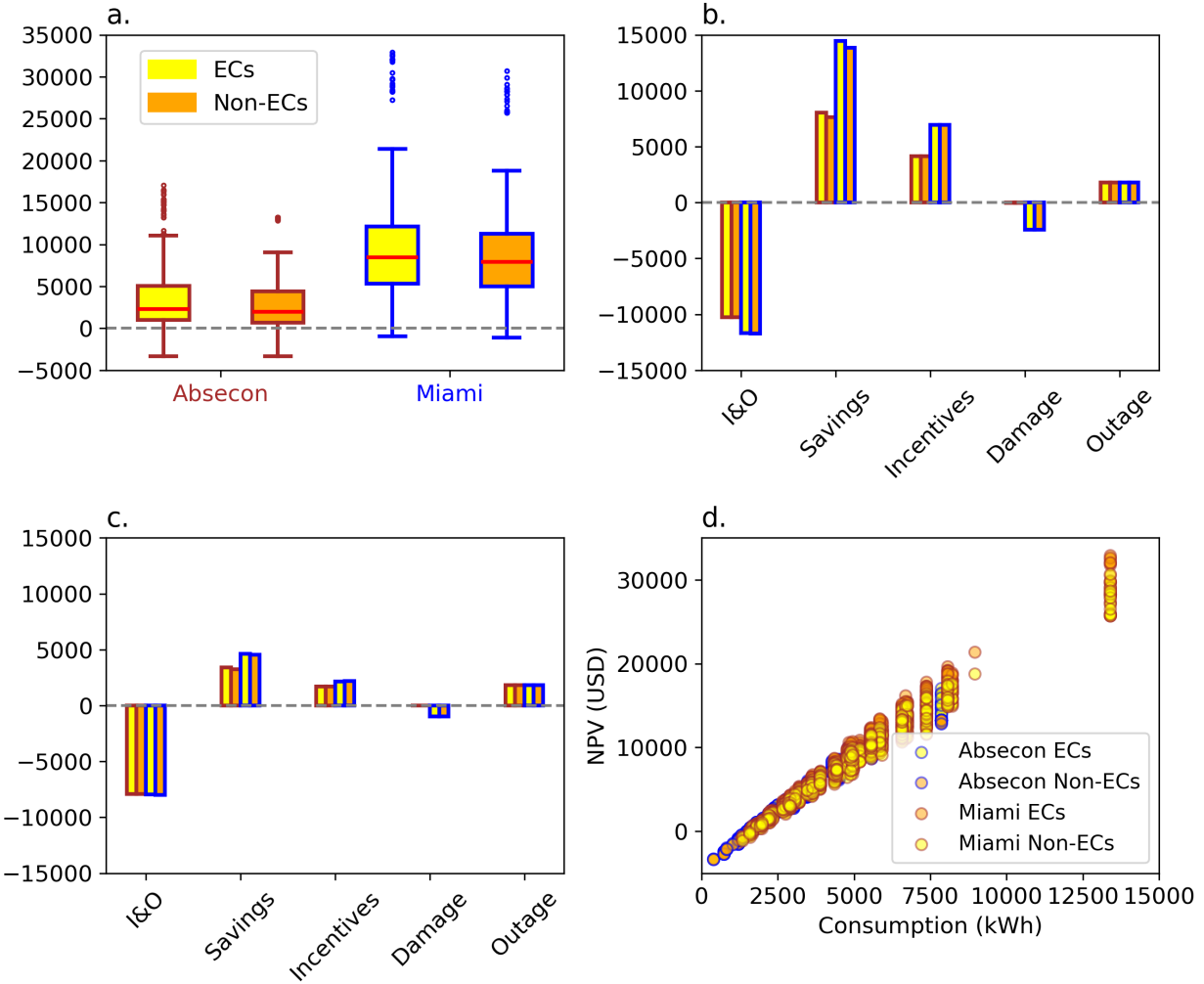


Fig. 6. **a.** NPV for each prosumer in Absecon City and Miami with state incentives. **b.** Average contributions of different components in NPV for profitable prosumers. **c.** Average contributions of different components in NPV for unprofitable prosumers. **d.** NPV vs. annual consumption for prosumers without state incentives.

281 We observe from Figure 6d that the NPV for prosumers increases with higher yearly consumption
 282 due to more significant savings from self-consumption. For example, in Absecon City, for ECs
 283 with state incentives, the mean yearly consumption of houses with positive NPV is 144% higher
 284 than that of houses with negative NPV. Similarly, in Miami, for ECs with state incentives, the mean
 285 yearly power consumption of prosumers with positive NPV is 141% higher than that of prosumers
 286 with negative NPV.

287 However, even unprofitable prosumers with a negative NPV can still gain significant electricity
 288 resilience. For instance, an unprofitable prosumer in Absecon City can still significantly reduce up
 289 to 20 hours in outage duration per year. This reduction can be up to 167 hours (~ 7 days) for an
 290 unprofitable prosumer in Miami. We present the cases of unprofitable prosumers with a negative
 291 NPV in Figure 6c. We find that lower savings (*e.g.*, 57% for unprofitable prosumers in Miami versus
 292 123% for profitable ones) contribute to a negative NPV. Solar panels are sized for net-zero energy
 293 consumption, and we assumed a constant battery size of 10kWh for all prosumers, leading to

294 higher ratios of I&O costs versus savings for smaller households. While batteries could be smaller
295 to reduce I&O costs [23], households would also lose resilience to more extended outages, e.g.,
296 outage lasted days for Hurricane Isaias [3]. Given these financial challenges, further research is
297 essential to better quantify the value of resilience that could significantly boost the adoption of
298 solar panels.

299 Meanwhile, to support solar adoption, incentives such as the 30% Solar Investment Tax Credit
300 (SITC) towards residential solar installations [67] and Successor Solar Incentive (SuSI) Program
301 [68] by NJ Clean Energy Programs can reduce the financial burden on households. As shown in
302 Figure 6d, state incentives can cover up to 40% and 60% of I&O costs for the profitable prosumers in
303 Absecon City and Miami. These incentives can significantly benefit the prosumers in low irradiance
304 regions, such as Absecon City, and could be crucial in helping unprofitable prosumers move toward
305 profitability. This is evident as there are only 26% profitable prosumers in Absecon City without
306 state incentives for ECs, while 80% profitable prosumers in Miami. These incentives will also attract
307 more solar panel adoption where net-metering rates are at wholesale rates, e.g., in New Jersey
308 [69], or where net-metering is expected to decrease to wholesale rates, e.g., in Florida with the
309 introduction of House Bill 741 [70].

310 Finally, we found that damage costs are negligible in Absecon City's low-wind region. In contrast,
311 in Miami's high winds region, the average damage cost over 25 years equals 21% of average I&O
312 costs. Miami's high-wind region experiences an annual mean panel failure rate of 3.3×10^{-2} , 21
313 times higher than 1.5×10^{-3} in Absecon. Despite this higher failure rate, solar panels can still
314 provide resilient electricity; for instance, when the chance of a panel failure is 3%, a class 7 pole
315 has a 38% chance of failure. The rate of solar panel damage was determined through hurricane
316 simulations and panel fragility assessments. Damage costs were calculated by multiplying the
317 failure rate by the cost of installing a new panel (see Methods). The "Solar Under Storm" report,
318 based on observations from hurricanes Irma and Maria in 2017 and Dorian in 2019, suggests
319 using vibration-resistant module bolted connections to enhance resilience. This would increase
320 installation costs by approximately 5%, which is still significantly lower than the 21% damage cost
321 [13]. Our results show Miami has more profitable prosumers even with approximately 100 times
322 higher damage costs than Absecon City because of higher solar irradiance. This highlights the need
323 for policies that not only incentivize solar adoption but also ensure resilience, enabling robust solar
324 energy even in high wind risk areas like Miami.

325 E. Community-scale resilience financing

326 The cost of installing new rooftop solar panels is covered by the individual house installing
327 the panels. However, the economic cost of undergrounding power lines is passed on to all the
328 consumers [38], requiring a financial analysis at the community scale, e.g., Florida Senate Bill 796
329 (2019) [71] (see methods). For a clean investment comparison of undergrounding versus ECs, we
330 analyzed NPVs at the community level, aggregating the cash flows for the 2,640 households.

331 At the community level, investments in ECs in Absecon City and Miami have positive aggregated
332 NPVs (Figure 7a). This positive NPV results from savings for the prosumers and reduced bills
333 for households without solar panels, who purchase electricity from prosumers at reduced prices.
334 Similar to NPV for individual prosumers, the NPV of the community in Miami is 188% higher than
335 the community in Absecon City with solar EC configuration.

336 In contrast, households primarily experience cash outflow during undergrounding due to
337 increased consumer bills needed to cover the cost, even though there is added value in resilience.
338 To cover the cost of undergrounding, households might observe an annual increase of up to 42%,
339 with the value of resilience being negligible in Absecon and only accounting for 0.3% of consumer
340 energy bills in Miami. Thus, we observe negative NPVs for the undergrounding of power lines in

341 both Absecon City and Miami in Figure 7a.

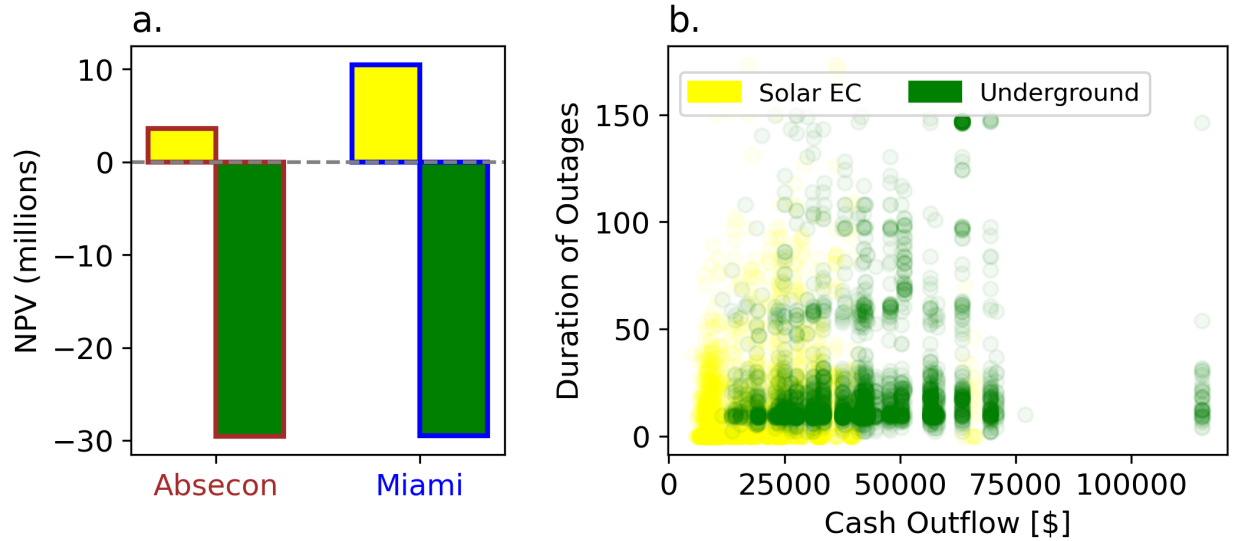


Fig. 7. Community-Scale Results. **a.** Community-wide NPV for adoption of solar panels in ECs and undergrounding cases. **b.** Scatter plot for the duration of outages and net cash outflow for ECs and undergrounding cases in Miami, Florida.

342 To compare each household’s total spending, we calculated the net cash outflow over the next
343 25 years for solar EC and undergrounding in the Miami region, including state incentives. We
344 calculated the net cash outflow because NPV includes savings that do not generate any cash inflow.
345 Although Absecon City had 92% profitable prosumers, close to 99% in Miami, we focused on Miami
346 due to its high wind region, where solar power significantly enhances community resilience. We
347 present the distribution of cashout flow and duration of outages for EC and undergrounding cases
348 for 2,640 households in Miami in Figure 7b. We observe a cluster of households in the community
349 with less than 50 hours of outages for ECs. In contrast, the undergrounding case has a higher
350 duration of outages. We observe that close to 16% of customers would experience more than 50
351 hours of outages in undergrounding case, whereas less than 8% would experience the same duration
352 in ECs. Battery backup, combined with more resilient solar panels, enhances the capacity of ECs to
353 operate in island mode. However, undergrounding 50% of power poles can still result in network
354 disconnections where poles remain above ground, leading to prolonged outages. The average cash
355 outflow of households in ECs is USD 16998.77 [7593.40 – 36012.95, 95%CI] while the average cash
356 outflow in the undergrounding case is 155% higher at USD 42552.67 [19164.34 – 69465.29, 95%CI].
357 Thus, ECs can gain more electricity resilience with lower net cash outflows than undergrounding
358 case.

359 3. DISCUSSION

360 We developed a high-fidelity outage risk model (Hi-Fi ORiM) of a power distribution network serv-
361 ing a city with 2,640 households. This model leverages multi-source datasets on roads, buildings
362 and power network and integrates state-of-the-art hurricane hazard model [27] to predict failures
363 of power network components, cascading outages, and recovery after hurricanes. We calibrated the
364 model to accurately reproduce outages from Hurricane Isaias (2020) in New Jersey [72], achieving
365 a 77.42% peak outage prediction compared to the actual 74.15% outages. Our validated risk model

366 represents a typical radial US power network. Thus, we used it as test bed for evaluating outage
367 risks and the feasibility (e.g., costs and benefits) of resilience measures across varying hurricane
368 conditions.

369 We studied resilience measures through four cases: a) No Upgrade, b) ECs, c) Non-ECs and
370 d) Undergrounding power lines. First, we analyzed how these resilience measures would have
371 enhanced electricity access for communities in Absecon City after Hurricane Isaias. We found
372 that ECs would have provided the most significant gains, with only 4.43% households facing
373 outages longer than 24hrs compared to 16.86%, 9.05%, and 8.41% for no upgrade, non-ECs, and
374 undergrounding cases, respectively.

375 We then investigated the benefits of these resilience measures for future hurricanes through
376 state-of-art disaster risk modeling. For a comprehensive analysis of hurricane conditions, we
377 extended our case study in Absecon City to include Miami, which, unlike Absecon City, is one of
378 the US regions facing the most significant hurricane hazards. Due to the higher hurricane hazards,
379 our predictions showed Miami could experience outage durations up to 100 times longer than
380 Absecon City.

381 We observed modest resilience gains in Absecon City for future hurricanes due to the lower
382 likelihood of experiencing many events like Hurricane Isaias. However, Miami is exposed to
383 stronger and more frequency hurricanes that can cause large-scale outages, and thus, we found
384 significant resilience gains. We predicted that Miami ECs would have average outage durations
385 64.4%, 33.0%, and 50.5% shorter than those in the no-upgrade, non-EC, and undergrounding cases,
386 respectively. We have already seen DERs can enhance electricity access after previous disasters.
387 Hurricane Ian in 2022 caused widespread outages, leaving 2.6 million households in Florida without
388 electricity. Nevertheless, Babcock Ranch, a small community in the state, maintained power for
389 2,000 households using its solar panels [5]. Similarly, after the Tohoku Earthquake in 2011, the
390 Sendai Microgrid continued to supply electricity through solar panels and batteries [73]. These
391 findings highlight the need for greater investment in DERs to bolster community resilience against
392 disasters. While the energy policies are shifting towards clean energy goals [74], they should also
393 focus on disaster risk management.

394 Next, we assessed the financial feasibility of implementing such resilience measures. We found
395 that the avoided costs from preventing outages are 18% and 23% of the investments and operations
396 (I&O) costs of these measures for profitable and unprofitable prosumers, respectively. To estimate
397 these avoided costs, we calculated the expenses of arranging alternate energy sources, such as
398 diesel generators, to access electricity during an outage. This approach results in different costs than
399 the typical small values of lost load (VoLL) from consumer surveys [43], traditional VoLL estimates
400 are not suited for disaster scenarios. Traditional VoLL underestimates the costs of outages, which
401 are based on hypothetical short outage scenarios [43]. We observe that unprofitable prosumers can
402 significantly reduce outage duration during hurricanes. This suggests that their financial feasibility
403 might be underestimated. Given these findings, future research should focus on quantifying the
404 true value of avoiding outages after disasters, as these prosumers might actually be profitable when
405 considering the broader economic benefits of resilience, especially for vulnerable groups relying on
406 electric medical equipment.

407 We also found that prosumers in Miami would observe a 21 times higher failure rate for solar
408 panels than prosumers in Absecon due to their higher wind hazards. Extensive structural sur-
409 veys after Hurricanes Irma (2017), Maria (2017), and Dorian (2019) found many rooftop panels
410 experienced failures in racks and clips attaching the panels to the racks in the Caribbean Islands
411 [13]. These surveys suggested vibration-resistant module bolted connections to improve resilience
412 against storm winds. Overall, the projected increase in solar installation cost is about 5% to gain
413 resilience through stronger structural systems. This projected cost is less than the expected damage

414 cost for solar panels in Miami for the next 25 years, which is 21% of I&O costs, including solar
415 panels and battery, and damage cost might be an even higher proportion of only solar panels costs.

416 We found that prosumers can be profitable with higher savings and incentives and that solar
417 adoption can also help the community become resilient. State incentives could be crucial in
418 determining consumers' willingness to adopt solar panels, especially in low-irradiance regions
419 such as New Jersey. Without state incentives, we found that the percentage of profitable prosumers
420 in Absecon City reduces from 92% to 26% for ECs as those incentives can cover up to 40% of I&O
421 cost. The reduction in profitable prosumers in Miami is not as drastic as in Absecon City, as regions
422 in Florida receive 25% more year-round consistent solar irradiance than in New Jersey. Moreover,
423 prosumers in ECs can earn more profit by selling excess solar power to local neighborhood energy
424 markets at higher selling costs than net-metering costs.

425 Unlike solar adoption, where only prosumers bear installment costs, undergrounding costs are
426 distributed among all households in the community. Therefore, we calculated the NPV for the
427 entire community for both ECs and undergrounding cases. ECs had a positive NPV for both
428 Absecon City and Miami, but the NPV was negative for the undergrounding case for both locations.
429 Consumers do not benefit financially from undergrounding, except for the added resilience, as it
430 mainly leads to increased electricity bills to cover the costs. We also compared the net cash outflow
431 (NCF) and duration of power outages for ECs and undergrounding cases in the Miami region for
432 25 years. The average NCF in undergrounding is 155% higher than in ECs. Moreover, more than
433 16% of the consumers would observe more than 50 hrs for power outage duration compared to less
434 than 8% of the consumers in ECs. Thus, adopting solar panels in the P2P sharing setting not only
435 increases the community's resilience benefits but also proves more profitable.

436 Finally, our study also has some limitations. Our Hi-Fi ORiM captures the structural failures
437 of the power grid components during hurricanes. However, this study does not consider the
438 synchronization of DERs with the main grid as required in IEEE Standard 1547-2018 [75]. Future
439 studies could address this limitation, as well as other requirements, such as voltage regulations,
440 since we only focus on the connectivity of power system components. Additionally, future research
441 could explore the value of inverters and the costs associated with operating a microgrid, especially
442 as additional operators might be required.

443 4. METHODS

444 A. High-Fidelity Outage Risk Model (Hi-Fi ORiM)

445 Researchers have developed probabilistic and machine-learning models to predict power outages
446 during a storm [51, 65, 76, 77], but these models only provide point estimates of the total number
447 of outages in a city and cannot quantify the risk at the component level for a power grid. Another
448 stream of literature has focused on developing synthetic grids to model the risk of natural disasters
449 to power networks as individual components have different hazard-dependent failure probabilities
450 [2, 31, 38, 78]. We developed a high-fidelity outage risk model (Hi-Fi ORiM) for the power network
451 to model hurricane risk to individual components (*e.g.*, poles, solar panels) at the residential level.
452 Our Hi-Fi ORiM was further employed to analyze mitigation strategies, such as rooftop solar
453 adoption and undergrounding power lines.

454 For this Hi-Fi ORiM model, we used open-source data for Absecon City, New Jersey, to create
455 a power network. We calibrated our Hi-Fi ORiM against outages recorded during Hurricane
456 Isaias (2020) by PowerOutage [72], as shown in Figure 2. To develop the synthetic power grid, we
457 calculated an average distance of approximately 60 meters between power poles, based on the
458 limited number of poles available in OpenStreetMap data [46]. We then used the roads shapefile
459 from New Jersey Geographic Information Network (NJGIN) [47] to place poles along five classes of

460 roads: US highways, state highways, county routes, other county roads, and local roads, excluding
 461 ramps and inaccessible roads (see Supplementary Text S1, Table S1, and Figures S1-S2). For
 462 simplicity, poles were positioned along the center of roads, and for two-way roads (*e.g.*, US and
 463 state highways), poles were placed on only one side. We obtained the locations of 2,640 residential
 464 buildings from New Jersey parcel data [48] and assigned each building to the nearest pole like a
 465 typical radial power grid. The power network can be represented as a graph $G = (N, E)$ where
 466 poles and houses are nodes (N), and connections between poles and from pole to houses are edges
 467 (E).

468 We captured the damage to the power distribution network through failures of power poles from
 469 hurricane winds. The probability of pole failure is hazard-dependent, *i.e.*, it changes with the wind
 470 and is represented through fragility curves for different classes of the pole (Figure 5c) obtained
 471 from [28]. The fragility curves are represented as.

$$P_f(w) = \phi\left(\frac{\ln(w/\bar{w})}{\beta}\right) \quad (1)$$

472 where $P_f(w)$ is the probability for an observed 3-second wind gust of $w \text{ ms}^{-1}$, $\phi(\cdot)$ is the standard
 473 normal distribution, \bar{w} is the median of fragility curves (*i.e.*, $P_f(\bar{w}) = 0.5$), and β is the dispersion
 474 parameter. The parameters \bar{w} and β vary depending on the class of the pole (Figure 1).

475 We used the tropical cyclone model from [27] to determine axis-symmetric winds and the
 476 background wind model from [53] to capture the complete wind structure. The historical hurricane
 477 paths are available from IBTRACS [79]. In [80], the authors emphasized the importance of using a
 478 complete wind structure, as excluding the background winds can result in underestimating wind
 479 hazards and, hence, an underprediction of risk from wind storms.

480 In [31], authors calibrated their synthetic grid for the poles of age 50 and 60 as most of the power
 481 distribution systems in the United States are old. We assumed a uniform age of 50 years for all
 482 poles in our synthetic power distribution network. We iteratively selected the class of pole for each
 483 road class from the seven available pole classes (Figure 1). We performed 1.6×10^6 iterations to
 484 select the combination of the class of poles, which minimizes the error on the predicted percentage
 485 of outages for our synthetic network with actually observed outages.

486 We obtained the observed percent of customers without power from PowerOutage[72]. Power-
 487 Outage reports the outages for all types of customers, including industrial, commercial, and
 488 residential. Since our focus is on residential customers, we matched only the percentage of cus-
 489 tomers without power, not the total number of customers affected. Additionally, PowerOutage
 490 compiles reports from utilities, which can delay the reporting of power outages [72]. Therefore, we
 491 assume that maximum outages occur initially and persist until a reported decrease in outages. To
 492 simulate total outages, we disconnected the network at identified failure points, forming subnet-
 493 works. Since transmission networks are predominantly aligned with US highways, we assumed
 494 that the subnetwork along the highway with the highest node density would retain power. The
 495 proportion of outages is given as.

$$O_{ratio} = \frac{\sum_{i=1}^{N_b} b_{oi}}{N_b} \quad (2)$$

496 where O_{ratio} is the percent of customers without power, $b_{oi} = 1$, if a building is disconnected
 497 from the supply network otherwise 0, and N_b is the total number of buildings. The final selection
 498 for pole classes was as follows: US and State Highways were assigned class 7 poles; County Routes
 499 were assigned class 3 poles; Other County Roads were assigned class 4 poles; and Local Roads
 500 were assigned class 5 poles.

501 We further calibrated our synthetic power distribution network to model the recovery time
 502 of failed poles. We assumed that repair teams would initially focus on main highways before
 503 progressing to local roads for restoration. In a radial network, this top-down strategy is expected to
 504 facilitate the rapid recovery of many buildings [62]. Therefore, we assigned recovery times to poles
 505 based on their distance from the US highway, formulated as follows.

$$t_{\text{recovery}} = \text{floor} \left(\frac{d}{100} \right) * t_1 + t_2 \quad (3)$$

506 where $\text{floor}(\cdot)$ is the greatest integer operator, d is the distance of a pole from the US highway in
 507 meters normalized with 100 meters, t_1 follows a truncated normal distribution as $t_1 \sim N(\bar{t}_1, \bar{t}_1/2)$,
 508 $t_1 \in (0, 2\bar{t}_1)$, and t_2 represents an initial time to start any repair work which also follows a truncated
 509 normal distribution, $t_2 \sim N(\bar{t}_2, \bar{t}_2/2)$, $t_2 \in (\bar{t}_2/2, 3\bar{t}_2/2)$. We calibrated \bar{t}_1 and \bar{t}_2 to represent the
 510 recovery during Hurricane Isaias (2020) (Figure 2b). Since recovery time depends on the number of
 511 failed poles, which is influenced by wind gusts in future hurricanes and constrained by the limited
 512 number of crews [62, 81], we scale \bar{t}_1 for a future hurricane, given as.

$$\bar{t}_{1 \text{ future}} = \frac{w_{\text{future}} \cdot \bar{t}_1}{w_{\text{Isaias}}} \quad (4)$$

513 where w_{future} is the 3-second wind gust of a future hurricane, and w_{Isaias} is the observed 3-second
 514 wind gust during hurricane Isaias.

515 We performed 400 uncertainty simulations for the scenario of hurricane Isaias and 4×10^5
 516 uncertainty simulations for future hurricanes. Each simulation begins by disconnecting the failed
 517 poles. Based on the recovery times, poles are reconnected to their original adjacent poles every
 518 hour. The simulation continues until all nodes in the original power network are fully restored.

519 B. Future Hurricanes

520 The 5,018 landfalling synthetic hurricanes chosen for this study consider the current climate
 521 scenario according to the National Center for Environmental Prediction (NCEP) reanalysis [44].
 522 The synthetic storm generative model involves three steps: random seeding for storm genesis, a
 523 beta-advection tropical cyclone motion model, and storm development based on environmental
 524 factors [44]. We show tracks of all synthetic hurricanes in Figure 5a.

525 On average, 3.38 landfalling hurricanes are expected per year in the US. Thus, the simulation of
 526 5,018 hurricanes corresponds to 1,485 years. We perform Monte-Carlo Simulations (MCS) [82] to
 527 determine the number of hurricanes in a year, assuming their occurrence follows a Poisson process,
 528 given as.

$$P(k) = e^{-\lambda} \frac{\lambda^k}{k!} \quad (5)$$

529 where $\lambda = 3.38/\text{yr}$ is average hurricane occurrences per year, and $P(k)$ is the probability of
 530 k number of hurricane events in an year. We randomly sampled without replacement yearly
 531 hurricanes for 1485 years from the dataset of 5018 synthetic storms. We represent a typical year
 532 with an average of 1485 years of simulation.

533 C. Solar Analysis

534 We used global horizontal irradiance (GHI), measured in watts per square meter units, to determine
 535 the total solar potential. We obtained the historical GHI from the National Solar Radiation Database,
 536 maintained by the National Renewable Energy Laboratory (NREL), which provides data at a spatial

537 resolution of $4km \times 4km$ and a temporal resolution of 30 minutes [29]. We averaged GHI over a
 538 window of 1 hour to obtain hourly GHI and used nearest-neighbor interpolation to assign GHI
 539 to the solar energy-generating building. While historical irradiance is available for the case of
 540 Hurricane Isaias (2020) scenario to measure the solar potential, we used solar irradiance for future
 541 hurricanes introduced by [26], which is given as.

$$I^h = \bar{I} \times e^{f(R,C)} \quad (6)$$

542 where I^h is the reduced irradiance during hurricane, \bar{I} is the spatiotemporal average of the
 543 observed irradiance, and $f(R, C) \leq 0$, is a function of the ratio of hurricane’s distance-to-site (d)
 544 to the radius-of-closed-isobars ($ROCI$) where winds are zero, $R = d/ROCI$ and category of a
 545 hurricane (C) as can be found in [26]. To calculate \bar{I} , we used the GHI at an hourly scale during
 546 2020 and averaged the irradiance at each hour across all days to get the \bar{I} for a typical 24-hour day
 547 of a month. We determined the start of outages and corresponding solar irradiance (I^h in Eq. 6) by
 548 using the location and month of the year for each hour from each synthetic hurricane’s genesis to
 549 its complete dissipation.

550 To share solar energy in ECs, we clustered houses using a k-means clustering algorithm based
 551 on Euclidean distance, with the average cluster containing ten houses. Refer to Supplementary
 552 Figure S8 for the distribution of the number of houses clustered together for energy sharing. We
 553 assumed that 50% of households in a cluster adopt solar panels and behind-the-meter batteries.
 554 Like overhead power lines, solar panels installed on rooftops are exposed to high hurricane winds.
 555 In [35], authors developed data-driven fragility models of the rooftop-mounted panels to the
 556 hurricane winds, represented similar to Eq. 1 with parameter $\bar{w} = 80 \text{ m/s}$ and $\beta = 0.32$.

557 We ran simulations for any pole and solar panel failures in our Hi-Fi ORiM during a hurricane.
 558 If a solar panel is damaged during a hurricane, only behind-the-meter power will provide the
 559 power during the disaster, and there will be no solar generation for that panel. Energy sharing
 560 during a disaster is only possible if none of the poles connecting houses in a cluster are damaged
 561 and all houses belong to the same disconnected subnetwork; otherwise, houses with solar panels
 562 will use the generated solar power for themselves. Also, during an emergency, households with
 563 solar panels first consume energy for themselves and then share any surplus equally with those
 564 without solar panels. We assume a simple power balance for household energy sharing but with
 565 no transmission losses [81]. Our study does not consider the failure of lines due to overloading
 566 [18], which could be addressed in future studies. Figure 8 outlines our approach to determining
 567 generated power.

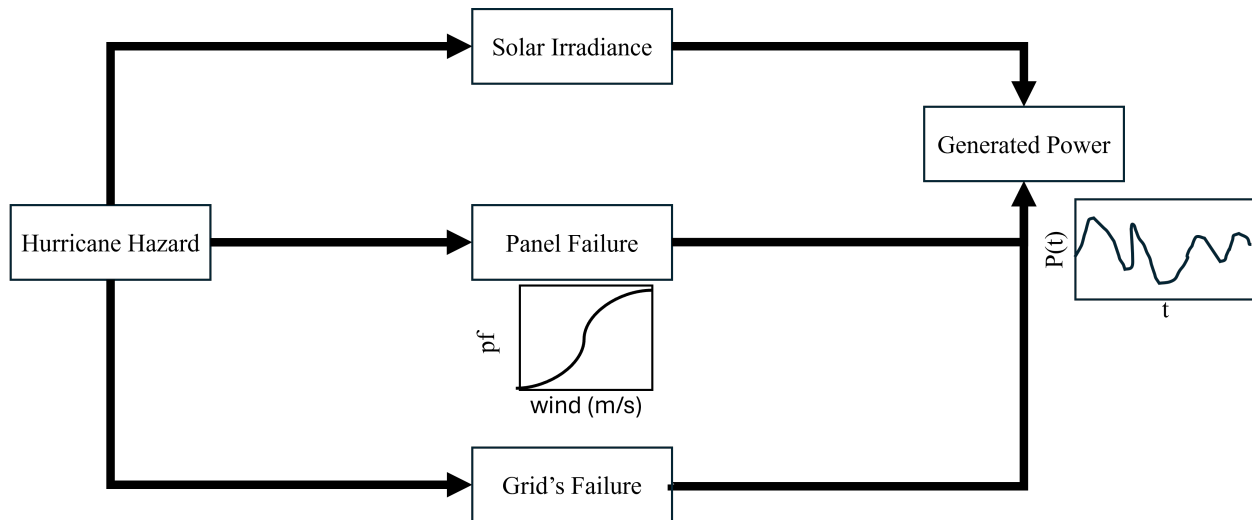


Fig. 8. Framework for evaluating the available energy during and after the hurricane. First, we get the cloud cover and winds during a hurricane. Then, we determine any failures for power poles and solar panels from hurricane winds. Finally, we determine the generated power during and after a hurricane.

568 We assumed that solar panels are made of standard crystal silicone with an energy conversion
 569 efficiency of 19% [33]. Further energy conversion losses could happen due to system losses such as
 570 soiling, shading, and wiring issues. Hence, we considered further system losses of 14%. Finally,
 571 we considered an AC-to-DC conversion ratio of 96%. Thus, the total available solar energy was
 572 calculated by multiplying GHI with the energy conversion efficiency, system losses, and AC-to-DC
 573 conversion factors [58].

574 For this study, rooftop solar panels are sized according to the net-zero energy efficiency crite-
 575 rion, meaning the total energy generated equals the total consumption by a house [25]. We also
 576 constrained the panel size not to exceed the roof area. We used open-source building footprints
 577 provided by Microsoft [49] to determine roof size.

578 Real-time electrical energy consumption data for individual buildings is not publicly available.
 579 However, NREL's ResStock provides a simulated dataset for thousands of residential load profiles
 580 across various climate zones in the United States [83]. These datasets are validated against the US
 581 Energy Information Administration's survey on residential energy use [84]. The load profile dataset
 582 includes buildings with different floor areas, construction years, and types, such as single-family
 583 and multi-family residential buildings.

584 We considered diverse load profiles since larger households typically consume more electricity,
 585 and newer houses might use electrical heating systems, unlike older buildings that often have
 586 gas-fired heaters [85]. The load profiles are available at the census block level across the US. Since
 587 our study focuses on residential buildings, we filtered the load profiles for single-family and
 588 multi-family residences based on census block, building area, and construction year. We obtained
 589 the construction year and number of floors from parcel data [48] and multiplied the number of
 590 floors by the building footprints [49] to calculate the total floor area for each building. Based on the
 591 different combinations of building floor area and year of construction (see Supplementary Text S2,
 592 Tables S2-S3, and Figure S6), we obtained consumption profiles for our synthetic grid at an hourly
 593 scale for a typical year.

594 D. Undergrounding

595 Undergrounding power lines can be an effective resilient strategy to hurricanes, as it reduces the
 596 exposure to the high hurricane winds [2, 39, 81]. Thus, we also investigated underground energy
 597 as an alternative to adopting solar energy to reduce cascading power blackouts during extreme
 598 weather events. We assume that 50% of the power lines to estimate the resilience gained with the
 599 undergrounding strategy. To understand the effect of undergrounding, we assume that power
 600 poles are undergrounding in the decreasing order of vulnerability. For example, class 7 poles are
 601 the most vulnerable (Figure 1), so they are assumed to be underground first. The poles for the
 602 underground power lines were assigned a zero probability of failure, *i.e.*, $P_f(w) \rightarrow 0$ in Eq. 1. The
 603 failure analysis and recovery for the rest of the poles in the synthetic grid are similar to methods
 604 for the synthetic grid without undergrounding.

605 E. Economics of resilience

606 Net present value (NPV) has been used to define prosumers' profitability. A positive NPV represents
 607 profit, while a negative NPV represents prosumers' losses. NPV is presented as.

$$NPV = -I_0 + \sum_{n=1}^{Lifetime} \left(\frac{CF}{(1+r)^n} \right) \quad (7)$$

608 where I_0 is the initial investment to install solar systems and behind-the-meter battery, the
 609 project's lifetime is 25 years, r is the discount rate, and CF is the cash flow, which is given as.

$$\begin{aligned} CF = & -C_{O\&M} - C_D - C_B(n = 11 \text{ or } n = 21) + P_{pv \rightarrow self} \times C_{grid} \\ & + P_{pv \rightarrow grid} \times C_{net-meter} + P_{pv \rightarrow local} \times C_{local} \\ & + P_{localpurchase} \times (C_{grid} - C_{local}) + D_{avoid-outage} \times C_{outage} \end{aligned} \quad (8)$$

610 where $C_{O\&M}$ is the cost of operation and maintenance, C_D is the cost of damage determined
 611 by multiplying the average failures of solar panels multiplied by the cost of installing a new
 612 panel, C_B is the cost of behind-the-meter battery assuming lifetime of a battery is 10 years, $P_{pv \rightarrow self}$
 613 is the self-consumption of solar power, $P_{pv \rightarrow local}$ is the surplus power sold locally, $P_{pv \rightarrow grid}$ is
 614 the surplus power sold to the grid, $P_{localpurchase}$ is the locally purchased electricity at the time of
 615 underproduction of solar power, C_{grid} is the cost of grid purchased electricity, $C_{net-meter}$ in the
 616 incentive from net-metering, C_{local} is the local sell price of electricity, $D_{avoid-outage}$ is the duration
 617 of avoided outages, and C_{outage} of avoided outage. Thus, $P_{pv \rightarrow self} \times C_{grid}$ represents the savings
 618 from self-consumption, $P_{pv \rightarrow grid} \times C_{net-meter} + P_{pv \rightarrow local} \times C_{local}$ represents the incentives from P2P
 619 sharing and net-metering, and $P_{localpurchase} \times (C_{grid} - C_{local})$ represents the savings by avoiding to
 620 the purchase the electricity from grid. We studied the case of ECs and non-ECs to understand the
 621 profit of selling electricity locally.

622 We calculated the cost of avoided outages by considering the reduction in outage duration with
 623 the adoption of solar panels in an average year (out of 1485 years of simulation). For our analysis,
 624 we determined the value of resilience by calculating the cost of an alternative energy source: a
 625 rental diesel generator. Consequently, the reduction in outages is rounded up to the nearest integer
 626 number of days to determine the rental cost for the diesel generator as the cost of avoided outages.

627 We also evaluate the NPV for the community in the solar EC community and undergrounding
 628 configurations of our synthetic power grid. We assume that the customers bear the cost of under-
 629 grounding, and the utility recovers the cost over the next 25 years. Thus, we distribute the cost

630 to the customers uniformly based on their annual consumption to their electricity bills, which is
 631 represented as.

$$\Delta C_{grid,underground} = \frac{I_{underground} - O_{underground}}{25 \times \sum P_{consumer}} \quad (9)$$

632 where $\Delta C_{grid,underground}$ is the increase in the bill of consumers, $I_{underground}$ is the cost of under-
 633 grounding, $O_{underground}$ is the reduction in operation cost of power lines after undergrounding, and
 634 $P_{consumer}$ is the energy consumption of each consumer. We use Eq. 7 and cash flow for underground-
 635 ing is.

$$CF_{underground} = -(C_{grid} + \Delta C_{grid,underground}) \times P_{consumer} + C_{outage,underground} \quad (10)$$

636 where $C_{outage,underground}$ is the cost of saved outages with the undergrounding risk mitigation
 637 strategy. We also compute the net cash outflow (NCF) for the mitigation strategies of solar EC and
 638 undergrounding. For undergrounding, NCF is given as.

$$NCF_{underground} = (C_{grid} + \Delta C_{grid,underground}) \times P_{consumer} \quad (11)$$

639 For solar EC, NCF is different for prosumers and consumers. For a prosumer, NCF is given as.

$$\begin{aligned} NCF_{solar,prosumer} = & I_0 + C_{O\&M} + C_D + C_B(n = 11 \text{ or } n = 21) - P_{pv \rightarrow self} \times C_{grid} \\ & - P_{pv \rightarrow grid} \times C_{net-meter} - P_{pv \rightarrow local} \times C_{local} \\ & + P_{localpurchase} \times C_{local} + P_{gridpurchase} \times C_{grid} \end{aligned} \quad (12)$$

640 NCF for a consumer is given as.

$$NCF_{solar,prosumer} = P_{localpurchase} \times C_{local} + P_{gridpurchase} \times C_{grid} \quad (13)$$

641 The Supplementary Text S3 provides all cost details used in the above calculations. Supplemen-
 642 tary Figure S10 presents an example of generated energy, energy sold, and energy purchased from
 643 the grid for a house with solar panels.

644 DATA AVAILABILITY

645 References for all the open-source data have been provided in the main manuscript, and data is
 646 available from authors upon reasonable request. Power outage data was obtained from Power-
 647 Outage [72]. We have also made available made the developed Hi-Fi ORiM risk model available at
 648 the NSF's DesignSafe repository at [86].

649 CODE AVAILABILITY

650 The code for hurricane risk simulation for the developed Hi-Fi ORiM is deposited to NSF's De-
 651 signSafe repository at [86]. Please contact the corresponding author for any queries related to the
 652 code.

653 ACKNOWLEDGEMENT

654 The authors are thankful for the financial support provided by the NYU Tandon School of Engineer-
 655 ing fellowship. The authors are also grateful to the support provided by NYU Center for Urban
 656 Science and Progress Dissertation Fellowship. This work was also supported in part through the
 657 NYU IT High Performance Computing resources, services, and staff expertise.

658 **COMPETING INTERESTS**

659 The authors have no competing interests.

660 **AUTHORS CONTRIBUTION**

661 P.A. and L.C. conceptualized the Hi-Fi ORiM and hurricane risk analysis framework. P.A. curated
662 the data and ran the simulations under the guidance of L.C. P.A. drafted the manuscript with
663 contributions and editing from L.C.

664 **REFERENCES**

- 665 1. Adam B. Smith. U.S. Billion-dollar Weather and Climate Disasters, 1980 - present (NCEI
666 Accession 0209268). *National Centers for Environmental Information*, 2020. doi: 10.25921/
667 STKW-7W73. URL <https://accession.nodc.noaa.gov/0209268>.
- 668 2. Kairui Feng, Min Ouyang, and Ning Lin. Tropical cyclone-blackout-heatwave compound
669 hazard resilience in a changing climate. *Nature Communications*, 13(1):1–11, 2022. ISSN 20411723.
670 doi: 10.1038/s41467-022-32018-4.
- 671 3. Mihir Zaveri and Ed Shanahan. Isaias Hits NY Area: 2.5 Million Lose Power and One Is Killed,
672 2020. URL <https://www.nytimes.com/2020/08/04/nyregion/isaias-ny.html>. The New York Times,
673 Accessed: 2024-08-30.
- 674 4. American Journal of Transportation. Hurricane Ida caused at least 1.2 million electricity
675 customers to lose power, 2021. URL [https://ajot.com/news/hurricane-ida-caused-at-least-1-
676 2-million-electricity-customers-to-lose-power](https://ajot.com/news/hurricane-ida-caused-at-least-1-2-million-electricity-customers-to-lose-power). Accessed: 2024-08-30.
- 677 5. Maria Cortes, Prateek Arora, Luis Ceferino, Haitham Ibrahim, Denis Istrati, Dorothy Reed,
678 David Roueche, Amir Safiey, Tori Tomoczek, Ioannis Zisis, Mohammad Alam, Tracy Kijewski-
679 Correa, David Prevatt, and Ian Robertson. StEER - Hurricane Ian, 2022. URL [https://doi.org/10.
680 17603/ds2-kc9k-s242](https://doi.org/10.17603/ds2-kc9k-s242). Accessed: 2024-08-30.
- 681 6. Alejandra Martinez and Emily Foxhall. Texas attorney general investigating centerpoint energy
682 after hurricane beryl’s long-lasting power outages. URL [https://www.texastribune.org/2024/07/
683 25/texas-power-grid-puc-centerpoint-hurricane-beryl/](https://www.texastribune.org/2024/07/25/texas-power-grid-puc-centerpoint-hurricane-beryl/). Accessed: 2024-08-31.
- 684 7. Paul M. Chakalian, Liza C. Kurtz, and David M. Hondula. After the Lights Go Out: Household
685 Resilience to Electrical Grid Failure Following Hurricane Irma. *Natural Hazards Review*, 20(4):
686 05019001, 2019. ISSN 1527-6988. doi: 10.1061/(asce)nh.1527-6996.0000335.
- 687 8. Kairui Feng, Min Ouyang, and Ning Lin. Hurricane-blackout-heatwave compound hazard
688 risk and resilience in a changing climate. *Nature Communications*, 13:4421, 2022. doi: 10.1038/
689 s41558-023-01596-6. URL <https://www.nature.com/articles/s41558-023-01596-6>.
- 690 9. Luis Ceferino, Judith Mitrani-Reiser, Anne Kiremidjian, Gregory Deierlein, and Celso Bam-
691 barén. Effective plans for hospital system response to earthquake emergencies. *Nature Commu-
692 nications* 2020 11:1, 11(1):1–12, 8 2020. ISSN 2041-1723. doi: 10.1038/s41467-020-18072-w. URL
693 <https://www.nature.com/articles/s41467-020-18072-w>.
- 694 10. Diana Mitsova, Ann Margaret Esnard, Alka Sapat, and Betty S. Lai. Socioeconomic vul-
695 nerability and electric power restoration timelines in Florida: the case of Hurricane Irma.
696 *Natural Hazards*, 94(2):689–709, 2018. ISSN 15730840. doi: 10.1007/s11069-018-3413-x. URL
697 <https://doi.org/10.1007/s11069-018-3413-x>.
- 698 11. National Academies of Sciences, Engineering, and Medicine. *Enhancing the Resilience of the
699 Nation’s Electricity System*. National Academies Press, July 2017. ISBN 978-0-309-46307-2. doi:
700 10.17226/24836.
- 701 12. Aleksandar M Stankovi, Kevin L Tomsovic, Fabrizio De Caro, Martin Braun, Joe H Chow, Ian
702 Dobson, Joseph Eto, Blair Fink, Christian Hachmann, David Hill, Chuanyi Ji, James A Kavicky,

- 703 Victor Levi, Chen-Ching Liu, Lamine Mili, Rodrigo Moreno, Mathaios Panteli, Frederic D Petit,
704 Giovanni Sansavini, Chanan Singh, Anurag K Srivastava, Kai Strunz, Hongbo Sun, Yin Xu,
705 and Shijia Zhao. Methods for Analysis and Quantification of Power System Resilience. *IEEE*
706 *TRANSACTIONS ON POWER SYSTEMS*, 38(5), 2023. doi: 10.1109/TPWRS.2022.3212688. URL
707 <https://doi.org/10.1109/TPWRS.2022.3212688>.
- 708 13. Laurie Stone. Solar Under Storm Part II: Designing Hurricane-Resilient PV Systems, 2020.
709 URL <https://rmi.org/solar-under-storm-part-ii-designing-hurricane-resilient-pv-systems/>. Accessed:
710 2024-09-03.
- 711 14. Katherine Antonio. Solar and wind to lead growth of U.S. power generation for the next two
712 years, 2024. URL <https://www.eia.gov/todayinenergy/detail.php?id=61242>. Accessed: 2024-09-03.
- 713 15. Chen Chen, Jianhui Wang, Feng Qiu, and Dongbo Zhao. Resilient Distribution System by
714 Microgrids Formation after Natural Disasters. *IEEE Transactions on Smart Grid*, 7(2):958–966, 3
715 2016. ISSN 19493053. doi: 10.1109/TSG.2015.2429653.
- 716 16. Gavin Newsom, David Carter, Doug Saucedo, Jim Zoellick, Charles Chamberlin, Marc Mar-
717 shall, Steve Shoemaker, Greg Chapman, Jana Ganion, Peter Lehman, Pramod Singh, Jamie
718 Patterson, Fernando Piña, and Drew Bohan. Demonstrating a secure, reliable, low-carbon com-
719 munity microgrid at the blue lake rancheria. Technical report, California Energy Commission,
720 2019. URL <https://www.schatzcenter.org>. CEC-500-2019-011.
- 721 17. Chao Long, Jianzhong Wu, Chenghua Zhang, Meng Cheng, and Ali Al-Wakeel. Feasibility of
722 Peer-to-Peer Energy Trading in Low Voltage Electrical Distribution Networks. *Energy Procedia*,
723 105:2227–2232, 5 2017. ISSN 1876-6102. doi: 10.1016/J.EGYPRO.2017.03.632.
- 724 18. Prakhar Mehta and Verena Tiefenbeck. Solar PV sharing in urban energy communities: Impact
725 of community configurations on profitability, autonomy and the electric grid. *Sustainable Cities*
726 *and Society*, 87:104178, 12 2022. ISSN 2210-6707. doi: 10.1016/J.SCS.2022.104178.
- 727 19. Esther Mengelkamp, Johannes Gärttner, Kerstin Rock, Scott Kessler, Lawrence Orsini, and
728 Christof Weinhardt. Designing microgrid energy markets: A case study: The Brooklyn
729 Microgrid. *Applied Energy*, 210:870–880, 1 2018. ISSN 0306-2619. doi: 10.1016/J.APENERGY.
730 2017.06.054.
- 731 20. U.S. Department of Energy. Puerto Rico Grid Recovery and Modernization, n.d.. URL
732 <https://www.energy.gov/gdo/puerto-rico-grid-recovery-and-modernization>. Accessed: 2024-08-30.
- 733 21. Kate Anderson, Nicholas D. Laws, Spencer Marr, Lars Lisell, Tony Jimenez, Tria Case, Xi-
734 angkun Li, Dag Lohmann, and Dylan Cutler. Quantifying and Monetizing Renewable
735 Energy Resiliency. *Sustainability 2018, Vol. 10, Page 933*, 10(4):933, 3 2018. ISSN 2071-
736 1050. doi: 10.3390/SU10040933. URL <https://www.mdpi.com/2071-1050/10/4/933/htmhttps://www.mdpi.com/2071-1050/10/4/933>.
- 738 22. Huangjie Gong and Dan M. Ione. Improving the Power Outage Resilience of Buildings
739 with Solar PV through the Use of Battery Systems and EV Energy Storage. *Energies 2021,*
740 *Vol. 14, Page 5749*, 14(18):5749, 9 2021. ISSN 1996-1073. doi: 10.3390/EN14185749. URL
741 <https://www.mdpi.com/1996-1073/14/18/5749/htmhttps://www.mdpi.com/1996-1073/14/18/5749>.
- 742 23. Travis Simpkins, Kate Anderson, Dylan Cutler, and Dan Olis. Optimal sizing of a solar-plus-
743 storage system for utility bill savings and resiliency benefits. *2016 IEEE Power and Energy*
744 *Society Innovative Smart Grid Technologies Conference, ISGT 2016*, 12 2016. doi: 10.1109/ISGT.
745 2016.7781237.
- 746 24. Jian Zhou, Stamatis Tsianikas, Dunbar P. Birnie, and David W. Coit. Economic and resilience
747 benefit analysis of incorporating battery storage to photovoltaic array generation. *Renewable*
748 *Energy*, 135:652–662, 5 2019. ISSN 0960-1481. doi: 10.1016/J.RENENE.2018.12.013.
- 749 25. Siddharth Patel, Luis Ceferino, Chenying Liu, Anne Kiremidjian, and Ram Rajagopal. The
750 disaster resilience value of shared rooftop solar systems in residential communities. *Earthquake*

- 751 *Spectra*, 37(4):2638–2661, 2021. ISSN 87552930. doi: 10.1177/87552930211020020.
- 752 26. Luis Ceferino, Ning Lin, and Dazhi Xi. Stochastic modeling of solar irradiance during hur-
753 ricanes. *Stochastic Environmental Research and Risk Assessment*, 36(9):2681–2693, 9 2022. ISSN
754 14363259. doi: 10.1007/S00477-021-02154-2/FIGURES/6. URL [https://link.springer.com/article/
755 10.1007/s00477-021-02154-2](https://link.springer.com/article/10.1007/s00477-021-02154-2).
- 756 27. Daniel R. Chavas, Ning Lin, and Kerry Emanuel. A model for the complete radial structure
757 of the tropical cyclone wind field. Part I: Comparison with observed structure. *Journal of the
758 Atmospheric Sciences*, 72(9):3647–3662, 2015. ISSN 15200469. doi: 10.1175/JAS-D-15-0014.1.
- 759 28. Yousef Mohammadi Darestani and Abdollah Shafieezadeh. Multi-dimensional wind fragility
760 functions for wood utility poles. *Engineering Structures*, 183:937–948, 3 2019. ISSN 0141-0296.
761 doi: 10.1016/J.ENGSTRUCT.2019.01.048.
- 762 29. Manajit Sengupta, Yu Xie, Anthony Lopez, Aron Habte, Galen Maclaurin, and James Shelby.
763 The National Solar Radiation Data Base (NSRDB). *Renewable and Sustainable Energy Reviews*, 89:
764 51–60, 6 2018. ISSN 1364-0321. doi: 10.1016/J.RSER.2018.03.003.
- 765 30. Luis Ceferino, Ning Lin, and Dazhi Xi. Modeling Solar Generation during Hurricanes. *Envi-
766 ronmental Science and Technology*, pages 1–28, 2021.
- 767 31. Chengwei Zhai, Thomas Ying jeh Chen, Anna Grace White, and Seth David Guikema. Power
768 outage prediction for natural hazards using synthetic power distribution systems. *Reliability
769 Engineering and System Safety*, 208(October 2020), 2021. ISSN 09518320. doi: 10.1016/j.res.2020.
770 107348.
- 771 32. Huangjie Gong. Models and Optimal Controls for Smart Homes and their Integration into the
772 Electric Power Grid. *Theses and Dissertations–Electrical and Computer Engineering*, 1 2022. doi:
773 <https://doi.org/10.13023/etd.2022.053>. URL https://uknowledge.uky.edu/ece_etds/179.
- 774 33. Aron P. Dobos. *PVWatts Version 5 Manual*, 2014. URL <https://www.nrel.gov/publications>.
- 775 34. Will Gorman, Galen Barbose, Juan Pablo Carvallo, Sunhee Baik, Chandler Miller, Philip White,
776 and Marlena Praprost. County-level assessment of behind-the-meter solar and storage to
777 mitigate long duration power interruptions for residential customers. *Applied Energy*, 342:
778 121166, 7 2023. ISSN 0306-2619. doi: 10.1016/J.APENERGY.2023.121166.
- 779 35. Luis Ceferino, Ning Lin, and Dazhi Xi. Bayesian updating of solar panel fragility curves and
780 implications of higher panel strength for solar generation resilience. *Reliability Engineering &
781 System Safety*, 229:108896, 1 2023. ISSN 0951-8320. doi: 10.1016/J.RESS.2022.108896.
- 782 36. Nicholas D. Laws, Kate Anderson, Nicholas A. DiOrio, Xiangkun Li, and Joyce McLaren.
783 Impacts of valuing resilience on cost-optimal PV and storage systems for commercial buildings.
784 *Renewable Energy*, 127:896–909, 11 2018. ISSN 0960-1481. doi: 10.1016/J.RENENE.2018.05.011.
- 785 37. Arkaprabha Bhattacharyya, Soojin Yoon, and Makarand Hastak. Optimal strategy selection
786 framework for minimizing the economic impacts of severe weather induced power outages.
787 *International Journal of Disaster Risk Reduction*, 60:102265, 6 2021. ISSN 2212-4209. doi: 10.1016/
788 J.IJDRR.2021.102265.
- 789 38. Zhecheng Wang, Michael Wara, Arun Majumdar, and Ram Rajagopal. Local and utility-
790 wide cost allocations for a more equitable wildfire-resilient distribution grid. *Nature Energy
791 2023 8:10*, 8(10):1097–1108, 8 2023. ISSN 2058-7546. doi: 10.1038/s41560-023-01306-8. URL
792 <https://www.nature.com/articles/s41560-023-01306-8>.
- 793 39. Julian Stürmer, Anton Plietzsch, Thomas Vogt, Frank Hellmann, Jürgen Kurths, Christian Otto,
794 Katja Frieler, and Mehrnaz Anvari. Increasing the resilience of the Texas power grid against ex-
795 treme storms by hardening critical lines. *Nature Energy 2024*, pages 1–10, 3 2024. ISSN 2058-7546.
796 doi: 10.1038/s41560-023-01434-1. URL <https://www.nature.com/articles/s41560-023-01434-1>.
- 797 40. Salim Moslehi and T. Agami Reddy. Sustainability of integrated energy systems: A
798 performance-based resilience assessment methodology. *Applied Energy*, 228:487–498, 10 2018.

- ISSN 0306-2619. doi: 10.1016/J.APENERGY.2018.06.075. URL <https://asu.pure.elsevier.com/en/publications/sustainability-of-integrated-energy-systems-a-performance-based-r>.
41. S. Ong, P. Denholm, and N. Clark. Grid parity for residential photovoltaics in the united states: Key drivers and sensitivities. Preprint, National Renewable Energy Laboratory (NREL), 2012. URL <https://www.osti.gov/bridge>. NREL/CP-6A20-54527, Presented at WREF 2012.
42. Kate Anderson, Amanda Farthing, Emma Elgqvist, and Adam Warren. Looking beyond bill savings to equity in renewable energy microgrid deployment. *Renewable Energy Focus*, 41: 15–32, 6 2022. ISSN 1755-0084. doi: 10.1016/J.REF.2022.02.001.
43. U.S. Department of Energy. Valuation of energy security for the united states (full report). Technical report, U.S. Department of Energy, 2017. URL [https://www.energy.gov/sites/prod/files/2017/01/f34/Valuation%20of%20Energy%20Security%20for%20the%20United%20States%20\(Full%20Report\)_1.pdf](https://www.energy.gov/sites/prod/files/2017/01/f34/Valuation%20of%20Energy%20Security%20for%20the%20United%20States%20(Full%20Report)_1.pdf). Accessed: 2024-08-30.
44. Reza Marsooli, Ning Lin, Kerry Emanuel, and Kairui Feng. Climate change exacerbates hurricane flood hazards along US Atlantic and Gulf Coasts in spatially varying patterns. *Nature Communications* 2019 10:1, 10(1):1–9, 8 2019. ISSN 2041-1723. doi: 10.1038/s41467-019-11755-z. URL <https://www.nature.com/articles/s41467-019-11755-z>.
45. Enrico Cicalò, Mara Balestrieri, Michele Valentino, Francesca Maria Ugliotti, Anna Osello, Muhammad Daud, and Ozan Onur Yilmaz. Enhancing Risk Analysis toward a Landscape Digital Twin Framework: A Multi-Hazard Approach in the Context of a Socio-Economic Perspective. *Sustainability* 2023, Vol. 15, Page 12429, 15(16):12429, 8 2023. ISSN 2071-1050. doi: 10.3390/SU151612429. URL <https://www.mdpi.com/2071-1050/15/16/12429/htm><https://www.mdpi.com/2071-1050/15/16/12429>.
46. OpenStreetMap contributors. OpenStreetMap. URL <https://www.openstreetmap.org/#map=5/38.007/-95.844>. Accessed: 2024-08-30.
47. New Jersey Geographic Information Network. Nj geographic information network: Roads dataset, . URL <https://njgin.nj.gov/njgin/edata/roads/>. Accessed: 2024-08-30.
48. New Jersey Geographic Information Network. Nj geographic information network: Parcels dataset, . URL <https://njgin.nj.gov/njgin/edata/parcels/index.html>. Accessed: 2024-08-30.
49. Microsoft. microsoft/USBuildingFootprints: Computer generated building footprints for the United States, 2018. URL <https://github.com/microsoft/USBuildingFootprints>. Accessed: 2024-08-30.
50. New Jersey Geographic Information Network. Nj geographic information network: Nj office of geographic information systems (njogis), . URL <https://njgin.nj.gov/njgin/about/ogis/>. Accessed: 2024-08-30.
51. Prateek Arora and Luis Ceferino. A Quasi-Binomial Regression Model for Hurricane-Induced Power Outages during Early Warning. *ASCE-ASME Journal of Risk and Uncertainty in Engineering Systems, Part A: Civil Engineering*, 10(2):04024027, 6 2024. ISSN 23767642. doi: 10.1061/AJRUA6.RUENG-1215/SUPPL{_}FILE/SUPPLEMENTAL{_}MATERIALS{_}{AJRUA6.RUENG-1215{_}ARORA.PDF. URL <https://ascelibrary.org/doi/abs/10.1061/AJRUA6.RUENG-1215><https://ascelibrary.org/doi/10.1061/AJRUA6.RUENG-1215>.
52. Prateek Arora and Luis Ceferino. Probabilistic and machine learning methods for uncertainty quantification in power outage prediction due to extreme events. *Natural Hazards and Earth System Sciences*, 23(5):1665–1683, 5 2023. ISSN 16849981. doi: 10.5194/NHESS-23-1665-2023.
53. Ning Lin, Kerry Emanuel, Michael Oppenheimer, and Erik Vanmarcke. Physically based assessment of hurricane surge threat under climate change. *Nature Climate Change*, 2(6): 462–467, 2012. ISSN 1758678X. doi: 10.1038/nclimate1389.
54. Andy Latto, Andrew Hagen, and Robbie Berg. National hurricane center tropical cyclone report: Hurricane isaias. Technical report, National Hurricane Center, June 2021. URL

- 847 https://www.nhc.noaa.gov/data/tcr/AL092020_Isaias.pdf.
- 848 55. American Society of Civil Engineers. ASCE 7 Standard: Minimum Design Loads and
849 Associated Criteria for Buildings and Other Structures, n.d. URL [https://www.asce.org/
850 publications-and-news/asce-7](https://www.asce.org/publications-and-news/asce-7). Accessed: 2024-08-30.
- 851 56. Jim Giuliano. Review and assessment of electric utility performance: August 4, 2020,
852 tropical storm isaias weather event. Technical report, New Jersey Board of Public Util-
853 ities, 2020. URL [https://www.nj.gov/bpu/pdf/boardorders/2020/20201118/6A%20-%202020%
854 20Tropical%20Storm%20Isaias%20BPU%20Staff%20Report.pdf](https://www.nj.gov/bpu/pdf/boardorders/2020/20201118/6A%20-%202020%20Tropical%20Storm%20Isaias%20BPU%20Staff%20Report.pdf). Division of Reliability and
855 Security.
- 856 57. U.S. Department of Energy. OE-417 Electric Emergency Incident and Disturbance Report Form.
857 URL <https://www.oe.netl.doe.gov/OE417/Form/Home.aspx>. Accessed: 2024-08-30.
- 858 58. Prateek Arora and Luis Ceferino. Could rooftop solar panels and storage have enhanced
859 the electricity resilience during Hurricane Isaias (2020)? *14th International Conference on
860 Applications of Statistics and Probability in Civil Engineering*, (2020), 2023.
- 861 59. U.S. Energy Information Administration. Annual Energy Outlook 2022. URL [https://www.eia.
862 gov/outlooks/aeo/data/browser/](https://www.eia.gov/outlooks/aeo/data/browser/). Accessed: 2024-08-31.
- 863 60. IEEE Standards Association. IEEE Standard 1366-2022: IEEE Guide for Electric Power Dis-
864 tribution Reliability Indices, 2022. URL <https://standards.ieee.org/ieee/1366/7243/>. Accessed:
865 2024-08-30.
- 866 61. Hao Wu, Xiangyi Meng, Michael M. Danziger, Sean P. Cornelius, Hui Tian, and Albert Lás-
867 zló Barabási. Fragmentation of outage clusters during the recovery of power distribu-
868 tion grids. *Nature Communications* 2022 13:1, 13(1):1–7, 11 2022. ISSN 2041-1723. doi:
869 10.1038/s41467-022-35104-9. URL <https://www.nature.com/articles/s41467-022-35104-9>.
- 870 62. Tara Walsh, Thomas Layton, David Wanik, and Jonathan Mellor. Agent Based Model to
871 Estimate Time to Restoration of Storm-Induced Power Outages. *Infrastructures* 2018, Vol. 3,
872 Page 33, 3(3):33, 8 2018. ISSN 2412-3811. doi: 10.3390/INFRASTRUCTURES3030033. URL
873 <https://www.mdpi.com/2412-3811/3/3/33/htmhttps://www.mdpi.com/2412-3811/3/3/33>.
- 874 63. NOAA Research. Hurricane Beryl: An opportunity for collaborative research, 2024. URL [https://
875 research.noaa.gov/2024/07/24/hurricane-beryl-an-opportunity-for-collaborative-research/](https://research.noaa.gov/2024/07/24/hurricane-beryl-an-opportunity-for-collaborative-research/). Ac-
876 cessed: 2024-08-30.
- 877 64. Kerry Manuel, Ragoth Sundararajan, and John Williams. Hurricanes and Global Warming:
878 Results from Downscaling IPCC AR4 Simulations. *Bulletin of the American Meteorological
879 Society*, 89(3):347–368, 3 2008. ISSN 0003-0007. doi: 10.1175/BAMS-89-3-347. URL [https://
880 journals.ametsoc.org/view/journals/bams/89/3/bams-89-3-347.xml](https://journals.ametsoc.org/view/journals/bams/89/3/bams-89-3-347.xml).
- 881 65. Seth David Guikema, Roshanak Nateghi, Steven M. Quiring, Andrea Staid, Allison C. Reilly,
882 and Michael Gao. Predicting Hurricane Power Outages to Support Storm Response Planning.
883 *IEEE Access*, 2(September 2015):1364–1373, 2014. ISSN 21693536. doi: 10.1109/ACCESS.2014.
884 2365716.
- 885 66. Kate Anderson, Eliza Hotchkiss, and Caitlin Murphy. Valuing resilience in electricity systems:
886 Quantifying, valuing, and monetizing its impact on system resilience. *Renewable Energy*, 2018.
887 doi: 10.1016/j.renene.2018.05.011. URL <https://doi.org/10.1016/j.renene.2018.05.011>.
- 888 67. U.S. Department of Energy. Homeowner’s guide to the federal tax
889 credit for solar photovoltaics, n.d.. URL [https://www.energy.gov/eere/solar/
890 homeowners-guide-federal-tax-credit-solar-photovoltaics](https://www.energy.gov/eere/solar/homeowners-guide-federal-tax-credit-solar-photovoltaics). Accessed: 2024-08-30.
- 891 68. New jersey’s clean energy successor solar incentives (susi) program: Administratively de-
892 termined incentive (adi) program revised srec-ii incentive levels. Technical report, New
893 Jersey Clean Energy Program, 2023. URL [https://njcleanenergy.com/renewable-energy/programs/
894 susi-program/adi-program](https://njcleanenergy.com/renewable-energy/programs/susi-program/adi-program).

- 895 69. New Jersey Clean Energy Program. Net Metering and Interconnection. URL <https://www.njcleanenergy.com/renewable-energy/programs/net-metering-and-interconnection>. Accessed: 2024-
896 08-31.
897
- 898 70. Florida Senate. House Bill 741 (2022) - Net Metering, 2022. URL <https://www.flsenate.gov/Session/Bill/2022/741>. Accessed: 2024-08-30.
899
- 900 71. Florida Senate. Senate Bill 796 (2019) - Public Utility Storm Protection Plans, 2019. URL
901 <https://www.flsenate.gov/Session/Bill/2019/796>. Accessed: 2024-08-30.
- 902 72. POWEROUTAGE.US. Poweroutage.us, 2020. URL <https://www.poweroutage.us>. Accessed:
903 2024-08-30.
- 904 73. Microgrids for Disaster Preparedness and Recovery, 2020. URL [https://preparecenter.org/
905 wp-content/sites/default/files/microgrids_for_disaster_prep_and_recovery.pdf](https://preparecenter.org/wp-content/sites/default/files/microgrids_for_disaster_prep_and_recovery.pdf). Accessed: 2024-09-
906 03.
- 907 74. Federal sustainability plan: Catalyzing america's clean energy industries and jobs. Technical
908 report, Office of the Federal Chief Sustainability Officer, 2021. URL [https://www.sustainability.
909 gov/pdfs/federal-sustainability-plan.pdf](https://www.sustainability.gov/pdfs/federal-sustainability-plan.pdf). Accessed: 2024-08-30.
- 910 75. IEEE Standards Association. IEEE Standard 1547-2018: IEEE Standard for Interconnection
911 and Interoperability of Distributed Energy Resources with Associated Electric Power Systems
912 Interfaces, 2018. URL <https://standards.ieee.org/ieee/1547/5915/>. Accessed: 2024-08-30.
- 913 76. Roshanak Nateghi, Seth Guikema, and Steven M. Quiring. Power Outage Estimation for
914 Tropical Cyclones: Improved Accuracy with Simpler Models. *Risk Analysis*, 34(6):1069–1078,
915 2014. ISSN 15396924. doi: 10.1111/risa.12131.
- 916 77. Sara Shashaani, Seth D. Guikema, Chengwei Zhai, Jordan V. Pino, and Steven M. Quiring.
917 Multi-Stage Prediction for Zero-Inflated Hurricane Induced Power Outages. *IEEE Access*, 6:
918 62432–62449, 2018. ISSN 21693536. doi: 10.1109/ACCESS.2018.2877078.
- 919 78. Adam B. Birchfield, Kathleen M. Gegner, Ti Xu, Komal S. Shetye, and Thomas J. Overbye.
920 Statistical Considerations in the Creation of Realistic Synthetic Power Grids for Geomagnetic
921 Disturbance Studies. *IEEE Transactions on Power Systems*, 32(2):1502–1510, 2017. ISSN 08858950.
922 doi: 10.1109/TPWRS.2016.2586460.
- 923 79. Kenneth R. Knapp, Michael C. Kruk, David H. Levinson, Howard J. Diamond, and Charles J.
924 Neumann. The international best track archive for climate stewardship (IBTrACS). *Bulletin
925 of the American Meteorological Society*, 91(3):363–376, 3 2010. ISSN 00030007. doi: 10.1175/
926 2009BAMS2755.1.
- 927 80. Prateek Arora and Luis Ceferino. A performance-based probabilistic framework to model risk
928 to power systems from hurricanes. *14th International Conference on Applications of Statistics and
929 Probability in Civil Engineering*, 2023.
- 930 81. Min Ouyang and Leonardo Dueñas-Osorio. Multi-dimensional hurricane resilience assessment
931 of electric power systems. *Structural Safety*, 48:15–24, 2014. ISSN 01674730. doi: 10.1016/j.
932 strusafe.2014.01.001. URL [http://dx.doi.org/10.1016/j.
933 strusafe.2014.01.001](http://dx.doi.org/10.1016/j.strusafe.2014.01.001).
- 934 82. Christopher Z Mooney. Introduction In: Monte Carlo Simulation. *Monte Carlo Simulation*,
935 pages 1–5, 1997. URL <http://methods.sagepub.com/book/monte-carlo-simulation/n1.xml>.
- 936 83. Eric J. H. Wilson, Andrew Parker, Anthony Fontanini, Elaina Present, Janet L. Reyna, Rajendra
937 Adhikari, Carlo Bianchi, Christopher CaraDonna, Matthew Dahlhausen, Janghyun Kim, Amy
938 LeBar, Lixi Liu, Marlena Praprost, Liang Zhang, Peter DeWitt, Noel Merket, Andrew Speake,
939 Tianzhen Hong, Han Li, Natalie Mims Frick, Zhe Wang, Aileen Blair, Henry Horsey, David
940 Roberts, Kim Trenbath, Oluwatobi Adekanye, Eric Bonnema, Rawad El Kontar, Jonathan
941 Gonzalez, Scott Horowitz, Dalton Jones, Ralph T. Muehleisen, Siby Platthotam, Matthew
942 Reynolds, Joseph Robertson, Kevin Sayers, and Qu Li. End-use load profiles for the u.s.
building stock: Methodology and results of model calibration, validation, and uncertainty

- 943 quantification. Technical report, National Renewable Energy Laboratory (NREL), Golden, CO
944 (United States), March 2022. URL <https://www.osti.gov/servlets/purl/1854582/>.
- 945 84. U.S. Energy Information Administration. Hurricane michael caused 1.7 million electricity
946 outages in the southeast united states, oct 2018. URL <https://www.eia.gov/todayinenergy/detail.php?id=37332>. Accessed: 2024-08-30.
- 948 85. Philip R. White, Joshua D. Rhodes, Eric J.H. Wilson, and Michael E. Webber. Quantifying the
949 impact of residential space heating electrification on the Texas electric grid. *Applied Energy*,
950 298:117113, 9 2021. ISSN 0306-2619. doi: 10.1016/J.APENERGY.2021.117113.
- 951 86. Prateek Arora and Luis Ceferino. Hurricane risk analysis of power failures, 2024. URL
952 <https://doi.org/10.17603/ds2-a510-6f83>.